Gradient schemes for two-phase flow in heterogeneous porous media and Richards equation

Robert Eymard, Cindy Guichard, Raphaèle Herbin, Roland Masson

▶ **To cite this version:**

Robert Eymard, Cindy Guichard, Raphaèle Herbin, Roland Masson. Gradient schemes for two-phase flow in heterogeneous porous media and Richards equation. Journal of Applied Mathematics and Mechanics / Zeitschrift für Angewandte Mathematik und Mechanik, 2013, Volume 94, Issue 7-8, p. 560-585, July 2014. 10.1002/zamm.201200206 . hal-00740367v3

HAL Id: hal-00740367
https://hal.science/hal-00740367v3

Submitted on 26 Jun 2013

HAL is a multi-disciplinary open access archive for the deposit and dissemination of scientific research documents, whether they are published or not. The documents may come from teaching and research institutions in France or abroad, or from public or private research centers.

L'archive ouverte pluridisciplinaire **HAL**, est destinée au dépôt et à la diffusion de documents scientifiques de niveau recherche, publiés ou non, émanant des établissements d'enseignement et de recherche français ou étrangers, des laboratoires publics ou privés.

Gradient schemes for two-phase flow in heterogeneous porous media and Richards equation

Robert Eymard[*], Cindy Guichard [†], Raphaèle Herbin [‡] and Roland Masson[§]

June 26, 2013

Abstract

The gradient scheme family, which includes the conforming and mixed finite elements as well as the mimetic mixed hybrid family, is used for the approximation of Richards equation and the two-phase flow problem in heterogeneous porous media. We prove the convergence of the approximate saturation and of the approximate pressures and approximate pressure gradients thanks to monotony and compactness arguments under an assumption of non-degeneracy of the phase relative permeabilities. Strong convergence results stem from the convergence of the norms of the gradients of pressures, which demand handling the nonlinear time term. Numerical results show the efficiency on these problems of a particular gradient scheme, called the Vertex Approximate Gradient scheme.

1 Introduction

We are interested here in the approximation of (u, v), solution to the incompressible two-phase flow problem in the space domain Ω over the time period $(0, T)$:

$$\Phi(\boldsymbol{x})\partial_t S(\boldsymbol{x}, p(\boldsymbol{x}, t)) - \mathrm{div}(k_1(\boldsymbol{x}, S(\boldsymbol{x}, p(\boldsymbol{x}, t)))\Lambda(\boldsymbol{x})(\nabla u(\boldsymbol{x}, t) + \boldsymbol{g}_1)) = f_1(\boldsymbol{x}, t), \tag{1a}$$

$$\Phi(\boldsymbol{x})\partial_t(1 - S(\boldsymbol{x}, p(\boldsymbol{x}, t))) - \mathrm{div}(k_2(\boldsymbol{x}, S(\boldsymbol{x}, p(\boldsymbol{x}, t)))\Lambda(\boldsymbol{x})(\nabla v(\boldsymbol{x}, t) + \boldsymbol{g}_2)) = f_2(\boldsymbol{x}, t), \tag{1b}$$

$$p(\boldsymbol{x}, t) = u(\boldsymbol{x}, t) - v(\boldsymbol{x}, t), \text{ for } (\boldsymbol{x}, t) \in \Omega \times (0, T), \tag{1c}$$

where u (resp. v) denotes the pressure of the phase 1, called the wetting phase (resp. of the phase 2, which is the nonwetting phase), p is the difference between the two pressures, called the capillary pressure, the saturation of the phase 1 is denoted by $S(\boldsymbol{x}, p)$ (it is called the "water content" in the framework of Richards' equation), and where Φ, Λ, k_i, $\boldsymbol{g}_i$ and f_i $(i = 1, 2)$ respectively denote the porosity, the absolute permeability, the mobility, the gravity and the source terms. Notice that the mobility k_i is defined as the ratio between the relative permeability and the viscosity, and that the gravity term $\boldsymbol{g}_i$ includes the density of the phase. Problem (1) is considered with the following initial condition:

$$S(\boldsymbol{x}, p(\boldsymbol{x}, 0)) = S(\boldsymbol{x}, p_{\mathrm{ini}}(\boldsymbol{x})), \text{ for a.e. } x \in \Omega, \tag{2}$$

together with the non-homogeneous Dirichlet boundary conditions:

$$u(\boldsymbol{x}, t) = \bar{u}(\boldsymbol{x}) \text{ and } v(\boldsymbol{x}, t) = \bar{v}(\boldsymbol{x}) \text{ on } \partial\Omega \times (0, T), \tag{3}$$

[*]L.A.M.A., UMR 8050, Université Paris-Est, France E-mail: Robert.Eymard@univ-mlv.fr

[†]L.J.A.D., UMR 7351, Université de Nice Sophia Antipolis & team Coffee INRIA Sophia Antipolis Méditerranée, France E-mail: Cindy.Guichard@unice.fr

[‡]Aix-Marseille Université, LATP, UMR 7353, 13453 Marseille, France E-mail: raphaele.herbin@univ-amu.fr

[§]L.J.A.D., UMR 7351, Université de Nice Sophia Antipolis E-mail: Roland.Masson@unice.fr

under the following assumptions:

- Ω is an open bounded connected polyhedral subset of $\mathbb{R}^d,\ d \in \mathbb{N}^\star$ and $T > 0$, (4a)
- Φ is a measurable function from Ω to $\mathbb{R}$ with $\Phi(\boldsymbol{x}) \in [\Phi_{\min}, \Phi_{\max}],\ \Phi_{\max} \geq \Phi_{\min} > 0$, (4b)
- Λ is a measurable function from Ω to $\mathcal{M}_d(\mathbb{R}),$ where $\mathcal{M}_d(\mathbb{R})$ denotes the set of $d \times d$ matrices, such that for a.e. $\boldsymbol{x} \in \Omega$, $\Lambda(\boldsymbol{x})$ is symmetric, and the set of its eigenvalues is included in $[\underline{\lambda}, \overline{\lambda}]$, with $0 < \underline{\lambda} \leq \overline{\lambda}$, (4c)
- $p_{\text{ini}} \in L^2(\Omega)$, (4d)
- $S(\boldsymbol{x}, q) \in [0,1]$ for all $(\boldsymbol{x}, q) \in \Omega \times \mathbb{R}$ with $S(\boldsymbol{x}, q) = S_j(q)$ for a.e. $\boldsymbol{x} \in \Omega_j$ and all $q \in \mathbb{R}$, where S_j is a non decreasing Lipschitz continuous function with constant $L_S,\ (\Omega_j)_{j\in J}$ is a family of disjoint connected polyhedral open sets such that $\bigcup_{j\in J} \overline{\Omega_j} = \overline{\Omega}$ where J is a finite set , (4e)
- $f_i \in L^2(\Omega \times (0,T)),\ i = 1,2,$ (4f)
- $k_i(\boldsymbol{x}, s) \in [k_{\min}, k_{\max}]$ for $(\boldsymbol{x}, s) \in \Omega \times [0,1]$ with $k_{\max} \geq k_{\min} > 0$ and $k_i(\cdot, s)$ measurable, $k_i(\boldsymbol{x}, \cdot)$ continuous, $i = 1,2,$ (4g)
- $\boldsymbol{g}_i \in \mathbb{R}^d,\ i = 1,2,$ (4h)
- $\bar{u}, \bar{v} \in H^1(\Omega)$. (4i)

Assumptions (4) are quite general, except for $k_{\min} > 0$ in Hypothesis (4g). This assumption is needed in the mathematical part of this paper (the influence of this parameter is studied numerically, see Section 5). Assumption (4e) is compatible with the so-called Van Genuchten model $S_j(p) = 1/((\max(-p,0)/p_j)^{n_j} + 1)^{m_j}$, with real parameters $p_j, n_j, m_j > 0$. The hypothesis that the function $S(\boldsymbol{x}, p)$ is defined by given functions in a partition of the domain is classical. Problem (1)-(2)-(3) is considered in this paper under the following weak sense.

$$
\begin{aligned}
&u - \bar{u}, v - \bar{v} \in L^2(0,T; H^1_0(\Omega)),\ p = u - v,\\
&\int_0^T \int_\Omega (-\Phi(\boldsymbol{x}) S(\boldsymbol{x}, p(\boldsymbol{x},t)) \partial_t \varphi(\boldsymbol{x},t) + k_1(\boldsymbol{x}, S(\boldsymbol{x}, p(\boldsymbol{x},t))) \Lambda(\boldsymbol{x})(\nabla u(\boldsymbol{x},t) + \boldsymbol{g}_1) \cdot \nabla \varphi(\boldsymbol{x},t))\, \mathrm{d}\boldsymbol{x}\mathrm{d}t\\
&- \int_\Omega \Phi(\boldsymbol{x}) S(\boldsymbol{x}, p_{\text{ini}}(\boldsymbol{x})) \varphi(\boldsymbol{x}, 0) \mathrm{d}\boldsymbol{x} = \int_0^T \int_\Omega f_1(\boldsymbol{x},t) \varphi(\boldsymbol{x},t) \mathrm{d}\boldsymbol{x}\mathrm{d}t,\ \forall \varphi \in C_c^\infty(\Omega \times [0,T)),\\
&\int_0^T \int_\Omega (\Phi(\boldsymbol{x}) S(\boldsymbol{x}, p(\boldsymbol{x},t)) \partial_t \varphi(\boldsymbol{x},t) + k_2(\boldsymbol{x}, S(\boldsymbol{x}, p(\boldsymbol{x},t))) \Lambda(\boldsymbol{x})(\nabla v(\boldsymbol{x},t) + \boldsymbol{g}_2) \cdot \nabla \varphi(\boldsymbol{x},t))\, \mathrm{d}\boldsymbol{x}\mathrm{d}t\\
&+ \int_\Omega \Phi(\boldsymbol{x}) S(\boldsymbol{x}, p_{\text{ini}}(\boldsymbol{x})) \varphi(\boldsymbol{x}, 0) \mathrm{d}\boldsymbol{x} = \int_0^T \int_\Omega f_2(\boldsymbol{x},t) \varphi(\boldsymbol{x},t) \mathrm{d}\boldsymbol{x}\mathrm{d}t,\ \forall \varphi \in C_c^\infty(\Omega \times [0,T)),
\end{aligned}
\tag{5}
$$

where we denote by $C_c^\infty(\Omega \times [0,T))$ the set of the restrictions of functions of $C_c^\infty(\Omega \times (-\infty, T))$ to $\Omega \times [0,T)$. Alternately, we also consider the case of Richards' equation, which can be obtained from (1) in two ways. One can replace (1a) by

$$u(\boldsymbol{x},t) = \bar{u}(\boldsymbol{x}) \text{ for } (\boldsymbol{x},t) \in \Omega \times (0,T), \tag{6}$$

or one can replace (1b) by

$$v(\boldsymbol{x},t) = \bar{v}(\boldsymbol{x}) \text{ for } (\boldsymbol{x},t) \in \Omega \times (0,T). \tag{7}$$

Then the corresponding weak formulation of the problem is obtained by replacing in (5) the first equation by (6) or the second one by (7). Note that this sense is an extension of the condition classically used in hydrogeological studies, which prescribes a constant condition with respect to time and space for the air pressure. As we show in the numerical examples, this extension allows to use Richards' equation as a good approximation of the full two phase flow problem in other engineering frameworks.

The existence of a weak solution to Problem (1), under various hypotheses, is studied in [2, 8, 12, 20] for example. Some mathematical results of convergence have been obtained for several approximations of this problem. Some

use the notion of global pressure, introduced by [10]; let us mention among these works the proof of convergence of a finite volume [21]. The standard finite volume scheme (based on a phase-by-phase upstream weighting), used in the petroleum engineering framework, was proven to converge in [19], and generalized in [5] in the case of discontinuous capillary pressures; in these works, the estimates on the approximate solutions are obtained thanks to the two-point flux approximation. Since our objective is the study of more general discretisation methods, we consider the formulation of the problem with two pressures, following [1]. The advantage of this formulation is that it includes both Richards problems (1b)-(6) or (1a)-(7) in the nonhomogeneous case.
Indeed, the purpose of this paper is to study the convergence of the so-called gradient schemes for the approximation of (5). These methods have been studied in [17] for linear elliptic problems, and in [14] in the case of nonlinear Leray-Lions-type elliptic and parabolic problems. The interest of the notion of gradient schemes is that it includes conforming finite elements with mass lumping (shown as efficient for linear [11], nonlinear [23] parabolic equations, and Richards type degenerate parabolic equations [9, 24]), mixed finite elements (applied to Richards' equation in [4]), hybrid mixed mimetic methods [13, 14], some discrete duality finite volume schemes, some particular Multi-point Flux Approximation and many other schemes. It is wellknown that the monotony properties which hold when using a two-point flux approximation are no longer true for more general schemes; this is the reason why Hypothesis (4g) is required in the mathematical study.
This paper is organized as follows. In Section 2, we recall the framework of gradient schemes which we use for the discretization of the problems under study. We then apply these schemes to Problem (1) in Section 3, and we prove the weak convergence of the approximate solutions. The corresponding scheme for Richards problems (1b)-(6) or (1a)-(7) is also studied. In Section 4, we improve this convergence by showing the strong convergence of the discrete pressures and pressure gradients. This analysis relies on an equation satisfied by a continuous solution, whose proof demands that some continuity properties with respect to time be satisfied. Numerical examples show the behaviour of the Vertex Approximate Gradient scheme, first introduced in [17], which presents some interesting characteristics for coupled flows in porous media (see Section 5). Let us emphasize that all the convergence results shown in this paper also hold in the case of Richards' problems.

2 Gradient schemes for diffusion problems

A gradient scheme can be viewed as a general nonconforming approximation of elliptic or parabolic problems. We begin with the discrete elements used for space partial differential equations.

Definition 2.1 (Gradient discretisation) *A gradient discretisation $\mathcal{D}$ for a space-dependent second order elliptic problem, with homogeneous Dririchlet boundary conditions, is defined by $\mathcal{D} = (X_\mathcal{D}, \Pi_\mathcal{D}, \nabla_\mathcal{D})$, where:*

1. *the set of discrete unknowns $X_\mathcal{D}$ is a finite dimensional vector space on $\mathbb{R}$, and $X_{\mathcal{D},0} \subset X_\mathcal{D}$ stands for the subspace of $X_\mathcal{D}$ devoted to the approximation of the homogeneous Dirichlet elliptic problem,*
2. *the linear mapping $\Pi_\mathcal{D} : X_\mathcal{D} \to L^2(\Omega)$ is the reconstruction of the approximate function,*
3. *the linear mapping $\nabla_\mathcal{D} : X_\mathcal{D} \to L^2(\Omega)^d$ is the discrete gradient operator. It must be chosen such that $\|\nabla_\mathcal{D} \cdot \|_{L^2(\Omega)^d}$ is a norm on $X_{\mathcal{D},0}$.*

Remark 2.2 *Let us notice that $\|\Pi_\mathcal{D} \cdot \|_{L^2(\Omega)}$ is not requested to be a norm on $X_{\mathcal{D},0}$. Indeed, in many examples that can be considered, some degrees of freedom are involved in the reconstruction of the gradient of the function, but not in that of the function itself.*

Definition 2.3 (Coercivity) *Let $\mathcal{D}$ be a gradient discretisation in the sense of Definition 2.1, and let $C_\mathcal{D}$ be the norm of the linear mapping $\Pi_\mathcal{D}$, defined by*

$$C_\mathcal{D} = \max_{v \in X_{\mathcal{D},0} \setminus \{0\}} \frac{\|\Pi_\mathcal{D} v\|_{L^2(\Omega)}}{\|\nabla_\mathcal{D} v\|_{L^2(\Omega)^d}}. \tag{8}$$

*A sequence $(\mathcal{D}_m)_{m\in\mathbb{N}}$ of gradient discretisations is said to be **coercive** if there exists $C_P \in \mathbb{R}_+$ such that $C_{\mathcal{D}_m} \leq C_P$ for all $m \in \mathbb{N}$.*

Remark 2.4 (Discrete Poincaré inequality.) *Equation* (8) *yields* $\|\Pi_{\mathcal{D}} v\|_{L^2(\Omega)} \leq C_{\mathcal{D}} \|\nabla_{\mathcal{D}} v\|_{L^2(\Omega)^d}$.

The consistency is ensured by a proper choice of the interpolation operator and discrete gradient.

Definition 2.5 (Consistency) *Let $\mathcal{D}$ be a gradient discretisation in the sense of Definition 2.1, and let $S_{\mathcal{D}} : H^1(\Omega) \to [0, +\infty)$ be defined by*

$$\forall \varphi \in H_0^1(\Omega)\,, \quad S_{\mathcal{D}}(\varphi) = \min_{v \in X_{\mathcal{D},0}} \left(\|\Pi_{\mathcal{D}} v - \varphi\|_{L^2(\Omega)} + \|\nabla_{\mathcal{D}} v - \nabla \varphi\|_{L^2(\Omega)^d} \right). \tag{9}$$

*A sequence $(\mathcal{D}_m)_{m \in \mathbb{N}}$ of gradient discretisations is said to be **consistent** if, for all $\varphi \in H_0^1(\Omega)$, $S_{\mathcal{D}_m}(\varphi)$ tends to 0 as $m \to \infty$.*

Since we are dealing with nonconforming methods, we require a "limit-conformity" of the method, i.e. that the dual of the discrete gradient be "close to" a discrete divergence in the following sense.

Definition 2.6 (Limit-conformity) *Let $\mathcal{D}$ be a gradient discretisation in the sense of Definition 2.1. We let $H_{\rm div}(\Omega) = \{\boldsymbol{\varphi} \in L^2(\Omega)^d, {\rm div}\boldsymbol{\varphi} \in L^2(\Omega)\}$ and $W_{\mathcal{D}}$: $H_{\rm div}(\Omega) \to [0, +\infty)$ be defined by*

$$\forall \boldsymbol{\varphi} \in H_{\rm div}(\Omega)\,,\ W_{\mathcal{D}}(\boldsymbol{\varphi}) = \max_{v \in X_{\mathcal{D},0} \setminus \{0\}} \frac{1}{\|\nabla_{\mathcal{D}} v\|_{L^2(\Omega)^d}} \left| \int_\Omega (\nabla_{\mathcal{D}} v(\boldsymbol{x}) \cdot \boldsymbol{\varphi}(\boldsymbol{x}) + \Pi_{\mathcal{D}} v(\boldsymbol{x}) {\rm div}\boldsymbol{\varphi}(\boldsymbol{x}))\, {\rm d}\boldsymbol{x} \right|. \tag{10}$$

*Note that for a conforming method such as the linear finite element method, one as $W_{\mathcal{D}}(\boldsymbol{\varphi}) = 0$. A sequence $(\mathcal{D}_m)_{m \in \mathbb{N}}$ of gradient discretisations is said to be **limit-conforming** if, for all $\boldsymbol{\varphi} \in H_{\rm div}(\Omega)$, $W_{\mathcal{D}_m}(\boldsymbol{\varphi})$ tends to 0 as $m \to \infty$.*

Dealing with generic non-linearity often requires compactness properties on the scheme.

Definition 2.7 (Compactness) *Let $\mathcal{D}$ be a gradient discretisation in the sense of Definition 2.1, and let $T_{\mathcal{D}} : \mathbb{R}^d \to \mathbb{R}^+$ be defined by*

$$\forall \boldsymbol{\xi} \in \mathbb{R}^d\,, \quad T_{\mathcal{D}}(\boldsymbol{\xi}) = \max_{v \in X_{\mathcal{D},0} \setminus \{0\}} \frac{\|\Pi_{\mathcal{D}} v(\cdot + \boldsymbol{\xi}) - \Pi_{\mathcal{D}} v\|_{L^2(\mathbb{R}^d)}}{\|\nabla_{\mathcal{D}} v\|_{L^2(\Omega)^d}} \tag{11}$$

where $\Pi_{\mathcal{D}} v$ has been extended by 0 outside Ω.
*A sequence $(\mathcal{D}_m)_{m \in \mathbb{N}}$ of gradient discretisations is said to be **compact** if the following uniform limit holds:*

$$\lim_{|\boldsymbol{\xi}| \to 0} \sup_{m \in \mathbb{N}} T_{\mathcal{D}_m}(\boldsymbol{\xi}) = 0.$$

Thanks to [17, Lemma 2.4], we may check the consistency and limit-conformity properties of given gradient schemes, using only dense subsets of the test function spaces.

Definition 2.8 (Space-time gradient discretisation) *Let Ω be an open subset of $\mathbb{R}^d$, with $d \in \mathbb{N}^\star$ and let $T > 0$ be given. We say that $\mathcal{D} = (X_{\mathcal{D}}, \Pi_{\mathcal{D}}, \nabla_{\mathcal{D}}, (t^{(n)})_{n=0,\ldots,N})$ is a space-time gradient discretisation of $\Omega \times (0,T)$ if*

- *$(X_{\mathcal{D}}, \Pi_{\mathcal{D}}, \nabla_{\mathcal{D}})$ is a gradient discretisation of Ω, in the sense of Definition 2.1,*
- *$t^{(0)} = 0 < t^{(1)} \ldots < t^{(N)} = T$.*

We then set $\delta t^{(n+\frac{1}{2})} = t^{(n+1)} - t^{(n)}$, for $n = 0, \ldots, N-1$, and $\delta t_{\mathcal{D}} = \max_{n=0,\ldots,N-1} \delta t^{(n+\frac{1}{2})}$.

Definition 2.9 (Space-time consistency) *A sequence $(\mathcal{D}_m)_{m \in \mathbb{N}}$ of space-time gradient discretisations of $\Omega \times (0,T)$, in the sense of Definition 2.8, is said to be **consistent** if it is consistent in the sense of Definition 2.5 and if $\delta t_{\mathcal{D}_m}$ tends to 0 as $m \to \infty$.*

Definition 2.10 (Piecewise constant function reconstruction)
Let $\mathcal{D} = (X_\mathcal{D}, \Pi_\mathcal{D}, \nabla_\mathcal{D}, (t^{(n)})_{n=0,\dots,N})$ be a space-time discretisation in the sense of Definition 2.8, and I be the finite set of the degrees of freedom, such that $X_\mathcal{D} = \mathbb{R}^I$. We say that $\Pi_\mathcal{D}$ is a piecewise constant function reconstruction if there exists a family of open subsets of Ω, denoted by $(K_i)_{i\in I}$, such that $\bigcup_{i\in I} \overline{K_i} = \overline{\Omega}$, $K_i \cap K_j = \emptyset$ for all $i \neq j$, and $\Pi_\mathcal{D} u = \sum_{i\in I} u_i \chi_{K_i}$ for all $u = (u_i)_{i\in I} \in X_\mathcal{D}$, where χ_{K_i} is the characteristic function of K_i.

Remark 2.11 *We do not require that there exists $j \in J$ such that $K_i \subset \Omega_j$.*

Remark 2.12 *An important example of space-time discretisation $\mathcal{D} = (X_\mathcal{D}, \Pi_\mathcal{D}, \nabla_\mathcal{D}, (t^{(n)})_{n=0,\dots,N})$ in the sense of Definition 2.8, such that $\Pi_\mathcal{D}$ is a piecewise constant function reconstruction in the sense of Definition 2.10, is the case of the mass-lumping of conforming finite elements. Indeed, assuming that $(\xi_i)_{i\in I}$ is the basis of some space $V_h \subset H^1_0(\Omega)$, we consider a family $(K_i)_{i\in I}$, chosen such that*

$$\|\sum_{i\in I} u_i \chi_{K_i} - \sum_{i\in I} u_i \xi_i\|_{L^2(\Omega)} \leq h \|\sum_{i\in I} u_i \nabla \xi_i\|_{L^2(\Omega)^d},\ \forall u \in X_\mathcal{D}.$$

We then define $\Pi_\mathcal{D}$ as in Definition 2.10, and $\nabla_\mathcal{D} u = \sum_{i\in I} u_i \nabla \xi_i$. In the case of the linear P^1 conforming finite element, the reconstruction is obtained by splitting each simplex in subsets defined by the highest barycentric coordinate, defining K_i as the union of the subsets of the simplices connected to the vertex indexed by i.

Remark 2.13 *Let $\mathcal{D} = (X_\mathcal{D}, \Pi_\mathcal{D}, \nabla_\mathcal{D}, (t^{(n)})_{n=0,\dots,N})$ be a space-time discretisation in the sense of Definition 2.8 such that $\Pi_\mathcal{D}$ is a piecewise constant function reconstruction in the sense of Definition 2.10. Note that we have the two important following properties:*

$$g(\Pi_\mathcal{D} u(\boldsymbol{x})) = \Pi_\mathcal{D} g(u)(\boldsymbol{x}),\ \text{for a.e. } \boldsymbol{x} \in \Omega,\ \forall u \in X_\mathcal{D},\ \forall g \in C(\mathbb{R}), \tag{12}$$

where for all continuous function $g \in C(\mathbb{R})$ and $u = (u_i)_{i\in I} \in X_\mathcal{D}$, we classically denote by $g(u) = (g(u_i))_{i\in I} \in X_\mathcal{D}$ and

$$\Pi_\mathcal{D} u(\boldsymbol{x}) \Pi_\mathcal{D} v(\boldsymbol{x}) = \Pi_\mathcal{D}(uv)(\boldsymbol{x}),\ \text{for a.e. } \boldsymbol{x} \in \Omega,\ \forall u, v \in X_\mathcal{D}, \tag{13}$$

where, for $u = (u_i)_{i\in I}$ and $v = (v_i)_{i\in I} \in X_\mathcal{D}$, we denote by $uv = (u_i v_i)_{i\in I} \in X_\mathcal{D}$.

3 Approximation of the two-phase flow problem by space-time gradient discretisations

Let $\mathcal{D} = (X_\mathcal{D}, \Pi_\mathcal{D}, \nabla_\mathcal{D}, (t^{(n)})_{n=0,\dots,N})$ be a space-time discretisation in the sense of Definition 2.8 such that $\Pi_\mathcal{D}$ is a piecewise constant function reconstruction in the sense of Definition 2.10. We define the following (implicit) scheme for the discretisation of Problem (5). We consider, for given $p^{(0)}, \bar{u}_\mathcal{D}, \bar{v}_\mathcal{D} \in X_\mathcal{D}$, a sequence $(u^{(n)}, v^{(n)})_{n=1,\dots,N} \subset X_\mathcal{D}$ such that:

$$s^{(0)}_\mathcal{D}(\boldsymbol{x}) = S(\boldsymbol{x}, \Pi_\mathcal{D} p^{(0)}(\boldsymbol{x})),\ p^{(n+1)} = u^{(n+1)} - v^{(n+1)} \tag{14a}$$

$$u^{(n+1)} - \bar{u}_\mathcal{D} \in X_{\mathcal{D},0},\ v^{(n+1)} - \bar{v}_\mathcal{D} \in X_{\mathcal{D},0}, \tag{14b}$$

$$s^{(n+1)}_\mathcal{D}(\boldsymbol{x}) = S(\boldsymbol{x}, \Pi_\mathcal{D} p^{(n+1)}(\boldsymbol{x})),\ \delta^{(n+\frac{1}{2})}_\mathcal{D} s_\mathcal{D}(\boldsymbol{x}) = \frac{s^{(n+1)}_\mathcal{D}(\boldsymbol{x}) - s^{(n)}_\mathcal{D}(\boldsymbol{x})}{\mathscr{t}^{(n+\frac{1}{2})}}, \tag{14c}$$

$$\int_\Omega \Big(\Phi(\boldsymbol{x}) \delta^{(n+\frac{1}{2})}_\mathcal{D} s_\mathcal{D}(\boldsymbol{x}) \Pi_\mathcal{D} w(\boldsymbol{x}) + k_1(\boldsymbol{x}, s^{(n+1)}_\mathcal{D}(\boldsymbol{x})) \Lambda(\boldsymbol{x}) (\nabla_\mathcal{D} u^{(n+1)}(\boldsymbol{x}) + \boldsymbol{g}_1) \cdot \nabla_\mathcal{D} w(\boldsymbol{x}) \Big) \mathrm{d}\boldsymbol{x}$$
$$= \frac{1}{\mathscr{t}^{(n+\frac{1}{2})}} \int_{t^{(n)}}^{t^{(n+1)}} \int_\Omega f_1(\boldsymbol{x}, t) \Pi_\mathcal{D} w(\boldsymbol{x}) \mathrm{d}\boldsymbol{x} \mathrm{d}t,\ \forall w \in X_{\mathcal{D},0},\ \forall n = 0, \dots, N-1, \tag{14d}$$

$$\int_\Omega \Big(-\Phi(\boldsymbol{x}) \delta^{(n+\frac{1}{2})}_\mathcal{D} s_\mathcal{D}(\boldsymbol{x}) \Pi_\mathcal{D} w(\boldsymbol{x}) + k_2(\boldsymbol{x}, s^{(n+1)}_\mathcal{D}(\boldsymbol{x})) \Lambda(\boldsymbol{x}) (\nabla_\mathcal{D} v^{(n+1)}(\boldsymbol{x}) + \boldsymbol{g}_2) \cdot \nabla_\mathcal{D} w(\boldsymbol{x}) \Big) \mathrm{d}\boldsymbol{x}$$
$$= \frac{1}{\mathscr{t}^{(n+\frac{1}{2})}} \int_{t^{(n)}}^{t^{(n+1)}} \int_\Omega f_2(\boldsymbol{x}, t) \Pi_\mathcal{D} w(\boldsymbol{x}) \mathrm{d}\boldsymbol{x} \mathrm{d}t,\ \forall w \in X_{\mathcal{D},0},\ \forall n = 0, \dots, N-1. \tag{14e}$$

We again use the notations $s_{\mathcal{D}}$, $\Pi_{\mathcal{D}}$ and $\nabla_{\mathcal{D}}$ for the definition of space-time dependent functions, defining

$$\begin{aligned}&s_{\mathcal{D}}(\boldsymbol{x},t) = s_{\mathcal{D}}^{(n+1)}(\boldsymbol{x}),\ \Pi_{\mathcal{D}}u(\boldsymbol{x},t) = \Pi_{\mathcal{D}}u^{(n+1)}(\boldsymbol{x}),\ \Pi_{\mathcal{D}}v(\boldsymbol{x},t) = \Pi_{\mathcal{D}}v^{(n+1)}(\boldsymbol{x})\\ &\text{and } \nabla_{\mathcal{D}}u(\boldsymbol{x},t) = \nabla_{\mathcal{D}}u^{(n+1)}(\boldsymbol{x}),\ \nabla_{\mathcal{D}}v(\boldsymbol{x},t) = \nabla_{\mathcal{D}}v^{(n+1)}(\boldsymbol{x}),\\ &\text{for a.e. } (\boldsymbol{x},t) \in \Omega \times (t^{(n)}, t^{(n+1)}),\ \forall n = 0,\dots,N-1.\end{aligned} \tag{15}$$

We also denote

$$\delta_{\mathcal{D}}s_{\mathcal{D}}(\boldsymbol{x},t) = \delta_{\mathcal{D}}^{(n+\frac{1}{2})}s_{\mathcal{D}}(\boldsymbol{x}),\ \text{for a.e. } (\boldsymbol{x},t) \in \Omega \times (t^{(n)}, t^{(n+1)}),\ \forall n = 0,\dots,N-1. \tag{16}$$

Remark 3.1 (The scheme for Richards' equation) *The scheme is obtained by Scheme* (14)*, replacing* (14d) *by* $u^{(n+1)} = \bar{u}_{\mathcal{D}}$ *or* (14e) *by* $v^{(n+1)} = \bar{v}_{\mathcal{D}}$.

In the proof of the lemma below and other lemmas later on, we shall make use of the function $\widetilde{S}$ defined by

$$\widetilde{S}(\boldsymbol{x},p) = \int_0^p qS'(\boldsymbol{x},q)\mathrm{d}q,\ \text{ for a.e. } \boldsymbol{x} \in \Omega,\ \forall p \in \mathbb{R}, \tag{17}$$

denoting by $S'(\boldsymbol{x},q) = S_j'(q)$ for a.e. $\boldsymbol{x} \in \Omega_j$, and all $q \in \mathbb{R}$ and $j \in J$. We also have

$$\widetilde{S}(\boldsymbol{x},p) = \widetilde{S}_j(p),\ \text{ for a.e. } \boldsymbol{x} \in \Omega_j,\ \forall p \in \mathbb{R},\ \text{with } \widetilde{S}_j(p) = \int_0^p qS_j'(q)\mathrm{d}q,\ \text{for } j \in J \text{ and } p \in \mathbb{R}. \tag{18}$$

Lemma 3.2 (Discrete $L^2(0,T;H_0^1(\Omega))$ estimate and existence of a discrete solution)
Under Hypotheses (4)*, let* $\mathcal{D} = (X_{\mathcal{D}}, \Pi_{\mathcal{D}}, \nabla_{\mathcal{D}}, (t^{(n)})_{n=0,\dots,N})$ *be a space-time gradient discretisation in the sense of Definition 2.8 such that* $\Pi_{\mathcal{D}}$ *is a piecewise constant function reconstruction in the sense of Definition 2.10. Then there exists at least one solution to Scheme* (14)*, and there exists* $C_1 > 0$*, only depending on the data introduced in Hypotheses* (4)*, on any* $C_P \in (0,+\infty)$ *greater than* $C_{\mathcal{D}}$ *(defined by* (8)*), and on* $\|\Pi_{\mathcal{D}}p^{(0)} - p_{\mathrm{ini}}\|_{L^2(\Omega)}$*,* $\|\Pi_{\mathcal{D}}\bar{u}_{\mathcal{D}} - \bar{u}\|_{L^2(\Omega)}$*,* $\|\Pi_{\mathcal{D}}\bar{v}_{\mathcal{D}} - \bar{v}\|_{L^2(\Omega)}$*,* $\|\nabla_{\mathcal{D}}\bar{u}_{\mathcal{D}} - \nabla\bar{u}\|_{L^2(\Omega)^d}$*,* $\|\nabla_{\mathcal{D}}\bar{v}_{\mathcal{D}} - \nabla\bar{v}\|_{L^2(\Omega)^d}$ *such that, for any solution* u, v *to this scheme,*

$$\|\nabla_{\mathcal{D}}u\|_{L^2(\Omega\times(0,T))^d} \le C_1 \text{ and } \|\nabla_{\mathcal{D}}v\|_{L^2(\Omega\times(0,T))^d} \le C_1. \tag{19}$$

Proof Let us first show (19). We take $w = \delta t^{(n+\frac{1}{2})}(u^{(n+1)} - \bar{u}_{\mathcal{D}})$ in (14d), $w = \delta t^{(n+\frac{1}{2})}(v^{(n+1)} - \bar{v}_{\mathcal{D}})$ in (14e), add the two such obtained equations and sum on $n = 0,\dots,N$. We get $T_1 + T_2 + T_3 = T_4 + T_5 + T_6$ with

$$T_1 = \sum_{n=0}^{N-1}\int_\Omega \Phi(\boldsymbol{x})(s_{\mathcal{D}}^{(n+1)}(\boldsymbol{x}) - s_{\mathcal{D}}^{(n)}(\boldsymbol{x}))\Pi_{\mathcal{D}}p^{(n+1)}(\boldsymbol{x})\mathrm{d}\boldsymbol{x},$$

$$T_2 = \int_0^T\int_\Omega k_1(\boldsymbol{x}, s_{\mathcal{D}}(\boldsymbol{x},t))\Lambda(\boldsymbol{x})\nabla_{\mathcal{D}}(u - \bar{u}_{\mathcal{D}})(\boldsymbol{x},t)\cdot\nabla_{\mathcal{D}}(u - \bar{u}_{\mathcal{D}})(\boldsymbol{x},t)\mathrm{d}\boldsymbol{x}\mathrm{d}t,$$

$$T_3 = \int_0^T\int_\Omega k_2(\boldsymbol{x}, s_{\mathcal{D}}(\boldsymbol{x},t))\Lambda(\boldsymbol{x})\nabla_{\mathcal{D}}(v - \bar{v}_{\mathcal{D}})(\boldsymbol{x},t)\cdot\nabla_{\mathcal{D}}(v - \bar{v}_{\mathcal{D}})(\boldsymbol{x},t)\mathrm{d}\boldsymbol{x}\mathrm{d}t,$$

$$\begin{aligned}T_4 = &\int_0^T\int_\Omega f_1(\boldsymbol{x},t)\Pi_{\mathcal{D}}(u - \bar{u}_{\mathcal{D}})(\boldsymbol{x},t)\mathrm{d}\boldsymbol{x}\mathrm{d}t\\ &- \int_0^T\int_\Omega k_1(\boldsymbol{x}, s_{\mathcal{D}}(\boldsymbol{x},t))\Lambda(\boldsymbol{x})(\nabla_{\mathcal{D}}\bar{u}_{\mathcal{D}}(\boldsymbol{x}) + \boldsymbol{g}_1)\cdot\nabla_{\mathcal{D}}(u - \bar{u}_{\mathcal{D}})(\boldsymbol{x},t)\mathrm{d}\boldsymbol{x}\mathrm{d}t,\end{aligned}$$

$$\begin{aligned}T_5 = &\int_0^T\int_\Omega f_2(\boldsymbol{x},t)\Pi_{\mathcal{D}}(v - \bar{v}_{\mathcal{D}})(\boldsymbol{x},t)\mathrm{d}\boldsymbol{x}\mathrm{d}t\\ &- \int_0^T\int_\Omega k_2(\boldsymbol{x}, s_{\mathcal{D}}(\boldsymbol{x},t))\Lambda(\boldsymbol{x})(\nabla_{\mathcal{D}}\bar{v}_{\mathcal{D}}(\boldsymbol{x}) + \boldsymbol{g}_2)\cdot\nabla_{\mathcal{D}}(v - \bar{v}_{\mathcal{D}})(\boldsymbol{x},t)\mathrm{d}\boldsymbol{x}\mathrm{d}t,\end{aligned}$$

and

$$T_6 = \sum_{n=0}^{N-1} \int_\Omega \Phi(\boldsymbol{x})(s_\mathcal{D}^{(n+1)}(\boldsymbol{x}) - s_\mathcal{D}^{(n)}(\boldsymbol{x}))\Pi_\mathcal{D}(\bar{u}_\mathcal{D} - \bar{v}_\mathcal{D})(\boldsymbol{x})\mathrm{d}\boldsymbol{x}.$$

With the definition (18), we have

$$0 \leq \widetilde{S}_j(p) \leq L_S \frac{p^2}{2}, \ \forall p \in \mathbb{R},$$

and, using the properties of the piecewise constant function $\Pi_\mathcal{D} p^{(n+1)}$, we can write

$$(s_\mathcal{D}^{(n+1)}(\boldsymbol{x}) - s_\mathcal{D}^{(n)}(\boldsymbol{x}))\Pi_\mathcal{D} p^{(n+1)}(\boldsymbol{x}) = \sum_{j\in J}\sum_{i\in I} \chi_{\Omega_j}(\boldsymbol{x})\chi_{K_i}(\boldsymbol{x})(S_j(p_i^{(n+1)}) - S_j(p_i^{(n)}))p_i^{(n+1)},$$

for a.e. $\boldsymbol{x} \in \Omega$. Since $\int_a^b qS_j'(q)\mathrm{d}q = \widetilde{S}_j(b) - \widetilde{S}_j(a) = b(S_j(b) - S_j(a)) - \int_a^b (S_j(q) - S_j(a))\mathrm{d}q$, we get that

$$(s_\mathcal{D}^{(n+1)}(\boldsymbol{x}) - s_\mathcal{D}^{(n)}(\boldsymbol{x}))\Pi_\mathcal{D} p^{(n+1)}(\boldsymbol{x}) \geq \sum_{j\in J}\sum_{i\in I} \chi_{\Omega_j}(\boldsymbol{x})\chi_{K_i}(\boldsymbol{x})(\widetilde{S}_j(p_i^{(n+1)}) - \widetilde{S}_j(p_i^{(n)})),$$

which leads to

$$T_1 \geq -\frac{\Phi_{\max} L_S}{2} \int_\Omega \sum_{j\in J}\sum_{i\in I} \chi_{\Omega_j}(\boldsymbol{x})\chi_{K_i}(\boldsymbol{x})(p_i^{(0)})^2 \mathrm{d}\boldsymbol{x} = -\frac{\Phi_{\max} L_S}{2} \|\Pi_\mathcal{D} p^{(0)}\|_{L^2(\Omega)}^2.$$

Thanks to Hypothesis (4c), we have

$$T_2 \geq \underline{\lambda} k_{\min} \|\nabla_\mathcal{D}(u - \bar{u}_\mathcal{D})\|_{L^2(\Omega\times(0,T))}^2,$$

and

$$T_3 \geq \underline{\lambda} k_{\min} \|\nabla_\mathcal{D}(v - \bar{v}_\mathcal{D})\|_{L^2(\Omega\times(0,T))}^2.$$

Applying the Cauchy-Schwarz inequality and (8), we get

$$T_4 \leq (C_\mathcal{D}\|f_1\|_{L^2(\Omega\times(0,T))} + k_{\max}\overline{\lambda}\sqrt{T}(\|\nabla_\mathcal{D}\bar{u}_\mathcal{D}\|_{L^2(\Omega)^d} + \sqrt{|\Omega|}|\boldsymbol{g}_1|))\|\nabla_\mathcal{D}(u - \bar{u}_\mathcal{D})\|_{L^2(\Omega\times(0,T))},$$

and

$$T_5 \leq (C_\mathcal{D}\|f_2\|_{L^2(\Omega\times(0,T))} + k_{\max}\overline{\lambda}\sqrt{T}(\|\nabla_\mathcal{D}\bar{v}_\mathcal{D}\|_{L^2(\Omega)^d} + \sqrt{|\Omega|}|\boldsymbol{g}_2|))\|\nabla_\mathcal{D}(v - \bar{v}_\mathcal{D})\|_{L^2(\Omega\times(0,T))}.$$

Thanks to the Young inequality, we get

$$T_4 \leq \frac{1}{2\underline{\lambda} k_{\min}}(C_\mathcal{D}\|f_1\|_{L^2(\Omega\times(0,T))} + k_{\max}\overline{\lambda}\sqrt{T}(\|\nabla_\mathcal{D}\bar{u}_\mathcal{D}\|_{L^2(\Omega)^d} + \sqrt{|\Omega|}|\boldsymbol{g}_1|))^2 + \frac{1}{2}T_2,$$

and

$$T_5 \leq \frac{1}{2\underline{\lambda} k_{\min}}(C_\mathcal{D}\|f_2\|_{L^2(\Omega\times(0,T))} + k_{\max}\overline{\lambda}\sqrt{T}(\|\nabla_\mathcal{D}\bar{v}_\mathcal{D}\|_{L^2(\Omega)^d} + \sqrt{|\Omega|}|\boldsymbol{g}_2|))^2 + \frac{1}{2}T_3.$$

We have

$$T_6 = \int_\Omega \Phi(\boldsymbol{x})(s_\mathcal{D}^{(N)}(\boldsymbol{x}) - s_\mathcal{D}^{(0)}(\boldsymbol{x}))\Pi_\mathcal{D}(\bar{u}_\mathcal{D} - \bar{v}_\mathcal{D})(\boldsymbol{x})\mathrm{d}\boldsymbol{x} \leq 2\Phi_{\max}\sqrt{|\Omega|}(\|\Pi_\mathcal{D}\bar{u}_\mathcal{D}\|_{L^2(\Omega)} + \|\Pi_\mathcal{D}\bar{v}_\mathcal{D}\|_{L^2(\Omega)}).$$

Gathering the above results shows (19). The existence of at least one solution is then easily proved by considering the function $S_\alpha(\boldsymbol{x}, q) = \alpha S(\boldsymbol{x}, q)$, for $\alpha \in [0,1]$, $\boldsymbol{x} \in \Omega$ and $q \in \mathbb{R}$, which ensures Hypotheses (4) as well. Since (19) holds for all $\alpha \in [0,1]$, and since the problem is linear for $\alpha = 0$, a classical topological degree argument provides the existence of at least one solution to Scheme (14). □ The following semi-norm, which is a discrete equivalent of a weighted $H^{-1}(\Omega)$ norm, will be useful in the control of the time translates in order to prove the strong convergence of $s_\mathcal{D}$.

Definition 3.3 (Dual semi-norm) *Under Hypotheses* (4)*, let $\mathcal{D} = (X_\mathcal{D}, \Pi_\mathcal{D}, \nabla_\mathcal{D})$ be a gradient discretisation of Ω in the sense of Definition 2.1. We define the following dual semi-norm on $L^2(\Omega)$:*

$$\forall w \in L^2(\Omega)\,,\ |w|_{\star,\mathcal{D}} = \sup\left\{\int_\Omega \Phi(\boldsymbol{x})w(\boldsymbol{x})\Pi_\mathcal{D}v(\boldsymbol{x})\mathrm{d}\boldsymbol{x}\ :\ v \in X_{\mathcal{D},0}, \|\nabla_\mathcal{D}v\|_{L^2(\Omega)^d} = 1\right\}. \tag{20}$$

Lemma 3.4 (Estimate on the dual semi-norm of the discrete time derivative of $s_\mathcal{D}$)
Under Hypotheses (4)*, let $\mathcal{D}$ be a space-time gradient discretisation in the sense of Definition 2.8. Let $u, v, s_\mathcal{D}$ be such that Scheme* (14) *holds. Then there exists C_2, only depending on the data introduced in Hypotheses* (4)*, on any $C_P \in (0, +\infty)$ greater than $C_\mathcal{D}$ (defined by* (8)*), and on $\|\Pi_\mathcal{D}p^{(0)} - p_{\rm ini}\|_{L^2(\Omega)}$, $\|\Pi_\mathcal{D}\bar{u}_\mathcal{D} - \bar{u}\|_{L^2(\Omega)}$, $\|\Pi_\mathcal{D}\bar{v}_\mathcal{D} - \bar{v}\|_{L^2(\Omega)}$, $\|\nabla_\mathcal{D}\bar{u}_\mathcal{D} - \nabla\bar{u}\|_{L^2(\Omega)^d}$, $\|\nabla_\mathcal{D}\bar{v}_\mathcal{D} - \nabla\bar{v}\|_{L^2(\Omega)^d}$, such that*

$$\int_0^T |\delta_\mathcal{D}s_\mathcal{D}(\cdot,t)|^2_{\star,\mathcal{D}}\mathrm{d}t \le C_2. \tag{21}$$

Proof Let us take $w \in X_{\mathcal{D},0}$ as test function in (14d). We have

$$\int_\Omega \Phi(\boldsymbol{x})\delta_\mathcal{D}^{(n+\frac12)}s_\mathcal{D}(\boldsymbol{x})\Pi_\mathcal{D}w(\boldsymbol{x})\mathrm{d}\boldsymbol{x} = -\int_\Omega k_1(\boldsymbol{x}, s_\mathcal{D}^{(n+1)}(\boldsymbol{x}))\Lambda(\boldsymbol{x})(\nabla_\mathcal{D}u^{(n+1)}(\boldsymbol{x}) + \boldsymbol{g}_1)\cdot\nabla_\mathcal{D}w(\boldsymbol{x})\mathrm{d}\boldsymbol{x}$$
$$+ \frac{1}{\delta t^{(n+\frac12)}}\int_{t^{(n)}}^{t^{(n+1)}}\int_\Omega f_1(\boldsymbol{x},t)\Pi_\mathcal{D}w(\boldsymbol{x})\mathrm{d}\boldsymbol{x}\mathrm{d}t,$$

which leads, thanks to (8), to

$$\int_\Omega \Phi(\boldsymbol{x})\delta_\mathcal{D}^{(n+\frac12)}s_\mathcal{D}(\boldsymbol{x})\Pi_\mathcal{D}w(\boldsymbol{x})\mathrm{d}\boldsymbol{x}$$
$$\le \left(k_{\max}\overline{\lambda}(\|\nabla_\mathcal{D}u^{(n+1)}\|_{L^2(\Omega)^d} + \sqrt{|\Omega|}|\boldsymbol{g}_1|) + \frac{C_\mathcal{D}}{\delta t^{(n+\frac12)}}\|\int_{t^{(n)}}^{t^{(n+1)}} f_1(\cdot,t)\mathrm{d}t\|_{L^2(\Omega)}\right)\|\nabla_\mathcal{D}w\|_{L^2(\Omega)^d}.$$

Taking the supremum on $w \in X_{\mathcal{D},0}$ such that $\|\nabla_\mathcal{D}w\|_{L^2(\Omega)^d} = 1$ gives an estimate on $|\delta_\mathcal{D}^{(n+\frac12)}s_\mathcal{D}|_{\star,\mathcal{D}}$. The proof is concluded by raising this estimate to the square, multiplying by $\delta t^{(n+\frac12)}$, summing on $n = 0, \ldots, N-1$ and estimating $\|\nabla_\mathcal{D}u\|_{L^2(\Omega\times(0,T))}$ thanks to Lemma 3.2. □

Lemma 3.5 (Relative compactness result) *Under Hypotheses* (4)*, let $(\mathcal{D}_m)_{m\in\mathbb{N}}$ be a consistent sequence of space-time gradient discretisations in the sense of Definition 2.9, such that the associated sequence of approximate gradient approximations is coercive (Definition 2.3), compact (Definition 2.7), and such that, for all $m \in \mathbb{N}$, $\Pi_{\mathcal{D}_m}$ is a piecewise constant function reconstruction in the sense of Definition 2.10. We assume that are given $p_m^{(0)}, \bar{u}_{\mathcal{D}_m}, \bar{v}_{\mathcal{D}_m} \in X_{\mathcal{D}_m}$ such that there exists $C_P > 0$ greater than $\|\Pi_{\mathcal{D}_m}p_m^{(0)} - p_{\rm ini}\|_{L^2(\Omega)}$, $\|\Pi_{\mathcal{D}_m}\bar{u}_{\mathcal{D}_m} - \bar{u}\|_{L^2(\Omega)}$, $\|\Pi_{\mathcal{D}_m}\bar{v}_{\mathcal{D}_m} - \bar{v}\|_{L^2(\Omega)}$, $\|\nabla_{\mathcal{D}_m}\bar{u}_{\mathcal{D}_m} - \nabla\bar{u}\|_{L^2(\Omega)^d}$, $\|\nabla_{\mathcal{D}_m}\bar{v}_{\mathcal{D}_m} - \nabla\bar{v}\|_{L^2(\Omega)^d}$, for all $m \in \mathbb{N}$. Let $u_m, v_m, s_{\mathcal{D}_m}$ be such that Scheme* (14) *holds for $m \in \mathbb{N}$.*
Then the family $(s_{\mathcal{D}_m})_{m\in\mathbb{N}}$ is relatively compact in $L^2(\Omega\times(0,T))$.

Proof Let us prolong the functions $s_{\mathcal{D}_m}$ by 0 outside of $\Omega\times(0,T)$. Let $\tau \in (0,T)$. We have, for $t \in (0, T-\tau)$,

$$\int_\Omega \Phi(\boldsymbol{x})(s_{\mathcal{D}_m}(\boldsymbol{x},t+\tau) - s_{\mathcal{D}_m}(\boldsymbol{x},t))^2\mathrm{d}\boldsymbol{x}$$
$$\le L_S\int_\Omega \Phi(\boldsymbol{x})(s_{\mathcal{D}_m}(\boldsymbol{x},t+\tau) - s_{\mathcal{D}_m}(\boldsymbol{x},t))(\Pi_{\mathcal{D}_m}p_m(\boldsymbol{x},t+\tau) - \Pi_{\mathcal{D}_m}p_m(\boldsymbol{x},t))\mathrm{d}\boldsymbol{x},$$

which provides, thanks to Definition 3.3 and taking the square root,

$$\sqrt{\Phi_{\min}}\|s_{\mathcal{D}_m}(\cdot,t+\tau) - s_{\mathcal{D}_m}(\cdot,t)\|_{L^2(\Omega)}$$
$$\le \sqrt{L_S}|s_{\mathcal{D}_m}(\cdot,t+\tau) - s_{\mathcal{D}_m}(\cdot,t)|^{1/2}_{\star,\mathcal{D}_m}\|\nabla_{\mathcal{D}_m}(p_m(t+\tau) - p_m(t))\|^{1/2}_{L^2(\Omega)^d}.$$

Thanks to the Young inequality and integrating on $(0, T-\tau)$, we get

$$\sqrt{\Phi_{\min}}\int_0^{T-\tau}\|s_{\mathcal{D}_m}(\cdot,t+\tau)-s_{\mathcal{D}_m}(\cdot,t)\|_{L^2(\Omega)}\mathrm{d}t \le \frac{\sqrt{L_S}}{2\sqrt{\tau}}\int_0^{T-\tau}|s_{\mathcal{D}_m}(\cdot,t+\tau)-s_{\mathcal{D}_m}(\cdot,t)|_{\star,\mathcal{D}_m}\mathrm{d}t + \frac{\sqrt{L_S\tau}}{2}\int_0^{T-\tau}\|\nabla_{\mathcal{D}_m}(p_m(t+\tau)-p_m(t))\|_{L^2(\Omega)^d}\mathrm{d}t.$$

We have, on one hand,

$$\int_0^{T-\tau}\|\nabla_{\mathcal{D}_m}(p_m(t+\tau)-p_m(t))\|_{L^2(\Omega)^d}\mathrm{d}t \le 2\int_0^T(\|\nabla_{\mathcal{D}_m}u_m(t)\|_{L^2(\Omega)}+\|\nabla_{\mathcal{D}_m}v_m(t)\|_{L^2(\Omega)})\mathrm{d}t,$$

and therefore

$$\int_0^{T-\tau}\|\nabla_{\mathcal{D}_m}(p_m(t+\tau)-p_m(t))\|_{L^2(\Omega)^d}\mathrm{d}t \le 2\sqrt{T}(\|\nabla_{\mathcal{D}_m}u_m\|_{L^2(\Omega\times(0,T))}+\|\nabla_{\mathcal{D}_m}v_m\|_{L^2(\Omega\times(0,T))}).$$

On the other hand, using the BV properties satisfied by piecewise constant functions, we have

$$\int_0^{T-\tau}|s_{\mathcal{D}_m}(\cdot,t+\tau)-s_{\mathcal{D}_m}(\cdot,t)|_{\star,\mathcal{D}_m}\mathrm{d}t \le \tau\int_0^T|\delta_{\mathcal{D}_m}s_{\mathcal{D}_m}(\cdot,t)|_{\star,\mathcal{D}_m}\mathrm{d}t,$$

which gives

$$\int_0^{T-\tau}|s_{\mathcal{D}_m}(\cdot,t+\tau)-s_{\mathcal{D}_m}(\cdot,t)|_{\star,\mathcal{D}_m}\mathrm{d}t \le \tau\sqrt{T}\left(\int_0^T|\delta_{\mathcal{D}_m}s_{\mathcal{D}_m}(\cdot,t)|^2_{\star,\mathcal{D}_m}\mathrm{d}t\right)^{1/2}.$$

Applying Lemmas 3.2 and 3.4, and using $0 \le s_{\mathcal{D}_m} \le 1$, we conclude to the existence of C_3, such that

$$\int_{\mathbb{R}}\|s_{\mathcal{D}_m}(\cdot,t+\tau)-s_{\mathcal{D}_m}(\cdot,t)\|_{L^2(\Omega)}\mathrm{d}t \le C_3\sqrt{|\tau|},\ \forall\tau\in\mathbb{R},$$

which provides, still using $0 \le s_{\mathcal{D}_m} \le 1$,

$$\int_{\mathbb{R}}\|s_{\mathcal{D}_m}(\cdot,t+\tau)-s_{\mathcal{D}_m}(\cdot,t)\|^2_{L^2(\Omega)}\mathrm{d}t \le C_3\sqrt{|\tau|}\sqrt{|\Omega|},\ \forall\tau\in\mathbb{R}.$$

Turning to the space translates, for all $\boldsymbol{\xi}\in\mathbb{R}^d$, let us define $\Omega_j^{(\boldsymbol{\xi})} = \{\boldsymbol{x}\in\Omega_j, \boldsymbol{x}+\boldsymbol{\xi}\in\Omega_j\}$. Thanks to the regularity hypothesis of $(\Omega_j)_{j\in J}$, then there exists $C_4>0$, only depending on $(\Omega_j)_{j\in J}$ such that

$$\sum_{j\in J}|\{\boldsymbol{x}\in\Omega_j, \boldsymbol{x}+\boldsymbol{\xi}\notin\Omega_j\}\cup\{\boldsymbol{x}\in\mathbb{R}^d\setminus\Omega_j, \boldsymbol{x}+\boldsymbol{\xi}\in\Omega_j\}| \le C_4|\boldsymbol{\xi}|,\ \forall\boldsymbol{\xi}\in\mathbb{R}^d.$$

Then, for a.e. $t\in(0,T)$, again using $0\le s_{\mathcal{D}_m}\le 1$,

$$\|s_{\mathcal{D}_m}(\cdot+\boldsymbol{\xi},t)-s_{\mathcal{D}_m}(\cdot,t)\|^2_{L^2(\mathbb{R}^d)} \le C_4|\boldsymbol{\xi}| + \sum_{j\in J}\|s_{\mathcal{D}_m}(\cdot+\boldsymbol{\xi},t)-s_{\mathcal{D}_m}(\cdot,t)\|^2_{L^2(\Omega_j^{(\boldsymbol{\xi})})},\ \forall\boldsymbol{\xi}\in\mathbb{R}^d.$$

We then remark that

$$\|s_{\mathcal{D}_m}(\cdot+\boldsymbol{\xi},t)-s_{\mathcal{D}_m}(\cdot,t)\|^2_{L^2(\Omega_j^{(\boldsymbol{\xi})})} = \int_{\Omega_j^{(\boldsymbol{\xi})}}(S_j(\Pi_{\mathcal{D}_m}p_m(\boldsymbol{x}+\boldsymbol{\xi},t))-S_j(\Pi_{\mathcal{D}_m}p_m(\boldsymbol{x},t)))^2\mathrm{d}\boldsymbol{x},$$

and therefore

$$\|s_{\mathcal{D}_m}(\cdot+\boldsymbol{\xi},t)-s_{\mathcal{D}_m}(\cdot,t)\|^2_{L^2(\Omega_j^{(\boldsymbol{\xi})})} \le L_S^2\int_{\mathbb{R}^d}(\Pi_{\mathcal{D}_m}p_m(\boldsymbol{x}+\boldsymbol{\xi},t)-\Pi_{\mathcal{D}_m}p_m(\boldsymbol{x},t))^2\mathrm{d}\boldsymbol{x}.$$

Using (11), we get

$$\|s_{\mathcal{D}_m}(\cdot+\boldsymbol{\xi},t)-s_{\mathcal{D}_m}(\cdot,t)\|^2_{L^2(\Omega_j^{(\boldsymbol{\xi})})}\leq L_S^2 T_{\mathcal{D}_m}(\boldsymbol{\xi})\|\nabla_{\mathcal{D}_m}p_m\|^2_{L^2(\Omega)^d}$$

Gathering the above results, we get

$$\int_0^T \|s_{\mathcal{D}_m}(\cdot+\boldsymbol{\xi},t)-s_{\mathcal{D}_m}(\cdot,t)\|^2_{L^2(\mathbb{R}^d)}\mathrm{d}t \leq TC_4|\boldsymbol{\xi}|+L_S^2T_{\mathcal{D}_m}(\boldsymbol{\xi})2(\|\nabla_{\mathcal{D}_m}u_m\|^2_{L^2(\Omega\times(0,T))}+\|\nabla_{\mathcal{D}_m}v_m\|^2_{L^2(\Omega\times(0,T))}).$$

Thanks to the compactness hypothesis (in the sense of Definition 2.7), we conclude that the $L^2(\mathbb{R}^d\times\mathbb{R})$ norm of $(s_{\mathcal{D}_m}-s_{\mathcal{D}_m}(\cdot+\boldsymbol{\xi},\cdot+\tau))_{m\in\mathbb{N}}$ uniformly tends to zero as $\boldsymbol{\xi},\tau\to 0$, which proves the relative compactness of the family in $L^2(\Omega\times(0,T))$. □

Lemma 3.6 (Minty trick) *Let ω be an open bounded subset of $\mathbb{R}^N$, $N\geq 1$, and let $S:\omega\times\mathbb{R}\to\mathbb{R}$ be a Caratheodory function, such that $S(\cdot,q)$ is measurable for all $q\in\mathbb{R}$ and $S(\boldsymbol{x},\cdot)$ is a nondecreasing function such that there exist $C>0$ with $|S(\boldsymbol{x},q)|\leq C$ for all $q\in\mathbb{R}$ and a.e. $\boldsymbol{x}\in\omega$. Let $(p_n)_{n\in\mathbb{N}}\subset L^2(\omega)$ such that*
(i) there exists $p\in L^2(\omega)$ such that $(p_n)_{n\in\mathbb{N}}$ weakly converges to p in $L^2(\omega)$;
(ii) there exists a function $\chi\in L^2(\omega)$ such that $(s_n)_{n\in\mathbb{N}}$ converges to χ in $L^2(\omega)$, where $s_n(\boldsymbol{x})=S(\boldsymbol{x},p_n(\boldsymbol{x}))$ for a.e. $\boldsymbol{x}\in\omega$.
Then $\chi(\boldsymbol{x})=S(\boldsymbol{x},p(\boldsymbol{x}))$, for a.e. $\boldsymbol{x}\in\omega$.

Proof We consider, for a given $q\in L^2(\omega)$,

$$A_n=\int_\omega (S(\boldsymbol{x},p_n(\boldsymbol{x}))-S(\boldsymbol{x},q(\boldsymbol{x})))(p_n(\boldsymbol{x})-q(\boldsymbol{x}))\mathrm{d}\boldsymbol{x}.$$

Since S is a nondecreasing, we have $A_n\geq 0$. By weak/strong convergence, we get that

$$\lim_{n\to\infty}A_n=\int_\omega(\chi(\boldsymbol{x})-S(\boldsymbol{x},q(\boldsymbol{x})))(p(\boldsymbol{x})-q(\boldsymbol{x}))\mathrm{d}\boldsymbol{x}\geq 0.$$

The above inequality holds in particular for $q=p-t\varphi$, with $t>0$ and $\varphi\in C_c^\infty(\omega)$. Then we get, dividing by $t>0$,

$$\int_\omega(\chi(\boldsymbol{x})-S(\boldsymbol{x},p(\boldsymbol{x})-t\varphi(\boldsymbol{x})))\varphi(\boldsymbol{x})\mathrm{d}\boldsymbol{x}\geq 0.$$

Letting $t\to 0$ in the above equation, we get, by dominated convergence, that

$$\int_\omega(\chi(\boldsymbol{x})-S(\boldsymbol{x},p(\boldsymbol{x})))\varphi(\boldsymbol{x})\mathrm{d}\boldsymbol{x}\geq 0.$$

Since the same inequality holds for $-\varphi$ instead of φ, we get

$$\int_\omega(\chi(\boldsymbol{x})-S(\boldsymbol{x},p(\boldsymbol{x})))\varphi(\boldsymbol{x})\mathrm{d}\boldsymbol{x}=0.$$

Since the above inequality holds for all $\varphi\in C_c^\infty(\omega)$, the conclusion of the lemma follows. □

Theorem 3.7 (Convergence of the numerical scheme) *Let Hypotheses* (4) *be fulfilled. Let $(\mathcal{D}_m)_{m\in\mathbb{N}}$ be a consistent sequence of space-time gradient discretisations in the sense of Definition 2.9, such that the associated sequence of approximate gradient approximations is coercive (Definition 2.3), limit–conforming (Definition 2.6) and compact (Definition 2.7), and such that, for all $m\in\mathbb{N}$, $\Pi_{\mathcal{D}_m}$ is a piecewise constant function reconstruction in the sense of Definition 2.10. We assume that are given $p_m^{(0)},\bar{u}_{\mathcal{D}_m},\bar{v}_{\mathcal{D}_m}\in X_{\mathcal{D}_m}$ such that the sequences $\|\Pi_{\mathcal{D}_m}p_m^{(0)}-p_{\rm ini}\|_{L^2(\Omega)}$, $\|\Pi_{\mathcal{D}_m}\bar{u}_{\mathcal{D}_m}-\bar{u}\|_{L^2(\Omega)}$, $\|\Pi_{\mathcal{D}_m}\bar{v}_{\mathcal{D}_m}-\bar{v}\|_{L^2(\Omega)}$, $\|\nabla_{\mathcal{D}_m}\bar{u}_{\mathcal{D}_m}-\nabla\bar{u}\|_{L^2(\Omega)^d}$, $\|\nabla_{\mathcal{D}_m}\bar{v}_{\mathcal{D}_m}-\nabla\bar{v}\|_{L^2(\Omega)^d}$ tend to 0 as $m\to\infty$. Let $u_m,v_m,s_{\mathcal{D}_m}$ be such that Scheme* (14) *holds for $m\in\mathbb{N}$.*
Then there exist $u,v\in L^2(\Omega\times(0,T))$ and $p=u-v$ such that, up to a subsequence,

1. $(\Pi_{\mathcal{D}_m} u_m, \Pi_{\mathcal{D}_m} v_m)$ *weakly converges in* $L^2(\Omega \times (0,T))^2$ *to* (u,v) *as* $m \to \infty$,
2. $(\nabla_{\mathcal{D}_m} u_m, \nabla_{\mathcal{D}_m} v_m)$ *weakly converges in* $(L^2(\Omega \times (0,T))^d)^2$ *to* $(\nabla u, \nabla v)$ *as* $m \to \infty$,
3. $s_{\mathcal{D}_m}$ *converges in* $L^2(\Omega \times (0,T))$ *to* s *such that* $s(\boldsymbol{x},t) = S(\boldsymbol{x}, p(\boldsymbol{x},t))$, *for a.e.* $(\boldsymbol{x},t) \in \Omega \times (0,T)$ *as* $m \to \infty$,

and (u,v) *is a weak solution of Problem* (5).

Proof Thanks to Lemmas 3.2 and 3.4, we first extract a subsequence such that the convergence results stated in Lemma 3.5 and 3.6 hold, as well as the three items of the above theorem. Let us now check that (u,v) is solution to (5). We first remark that $u - \bar{u} \in L^2(0,T; H_0^1(\Omega))$, since, prolonging this function by 0 outside of $\Omega \times (0,T)$, we get that $\nabla u - \nabla \bar{u} \in L^2(\mathbb{R}^d \times (0,T))$ using the limit-conformity of the sequence of discretisations. The same holds for $v - \bar{v}$.

Let $m \in \mathbb{N}$, and let us denote $\mathcal{D} = \mathcal{D}_m$ (belonging to the above subsequence) and drop some subscripts m for the simplicity of the notation.

Let $\varphi \in C_c^\infty([0,T))$ and $w \in C_c^\infty(\Omega)$, and let $w_\mathcal{D} \in X_{\mathcal{D},0}$ be such that

$$w_\mathcal{D} = \operatorname*{argmin}_{z \in X_{\mathcal{D},0}} \left(\|\Pi_\mathcal{D} z - w\|_{L^2(\Omega)} + \|\nabla_\mathcal{D} z - \nabla w\|_{L^2(\Omega)^d} \right).$$

We take $\delta t^{(n+\frac{1}{2})} \varphi(t^{(n)}) w_\mathcal{D}$ as test function in (14d), and we sum the resulting equation on $n = 0, \dots, N-1$. We get

$$T_7^{(m)} + T_8^{(m)} = T_9^{(m)}, \tag{22}$$

with

$$T_7^{(m)} = \sum_{n=0}^{N-1} \delta t^{(n+\frac{1}{2})} \varphi(t^{(n)}) \int_\Omega \Phi(\boldsymbol{x}) \delta_\mathcal{D}^{(n+\frac{1}{2})} s_\mathcal{D}(\boldsymbol{x}) \Pi_\mathcal{D} w_\mathcal{D}(\boldsymbol{x}) \mathrm{d}\boldsymbol{x},$$

$$T_8^{(m)} = \sum_{n=0}^{N-1} \delta t^{(n+\frac{1}{2})} \varphi(t^{(n)}) \int_\Omega k_1(\boldsymbol{x}, s_\mathcal{D}^{(n+1)}(\boldsymbol{x})) \Lambda(\boldsymbol{x}) (\nabla_\mathcal{D} u^{(n+1)}(\boldsymbol{x}) + \boldsymbol{g}_1) \cdot \nabla_\mathcal{D} w_\mathcal{D}(\boldsymbol{x}) \mathrm{d}\boldsymbol{x},$$

and

$$T_9^{(m)} = \sum_{n=0}^{N-1} \varphi(t^{(n)}) \int_{t^{(n)}}^{t^{(n+1)}} \int_\Omega f_1(\boldsymbol{x},t) \Pi_\mathcal{D} w_\mathcal{D}(\boldsymbol{x}) \mathrm{d}\boldsymbol{x} \mathrm{d}t.$$

Writing

$$T_7^{(m)} = -\int_0^T \varphi'(t) \int_\Omega \Phi(\boldsymbol{x}) s_\mathcal{D}(\boldsymbol{x},t) \Pi_\mathcal{D} w_\mathcal{D}(\boldsymbol{x}) \mathrm{d}\boldsymbol{x} \mathrm{d}t - \varphi(0) \int_\Omega \Phi(\boldsymbol{x}) S(\boldsymbol{x}, \Pi_\mathcal{D} p_m^{(0)}(\boldsymbol{x})) \Pi_\mathcal{D} w_\mathcal{D}(\boldsymbol{x}) \mathrm{d}\boldsymbol{x},$$

we get that

$$\lim_{m \to \infty} T_7^{(m)} = -\int_0^T \varphi'(t) \int_\Omega \Phi(\boldsymbol{x}) s(\boldsymbol{x},t) w(\boldsymbol{x}) \mathrm{d}\boldsymbol{x} \mathrm{d}t - \varphi(0) \int_\Omega S(\boldsymbol{x}, p_{\mathrm{ini}}(\boldsymbol{x})) w(\boldsymbol{x}) \mathrm{d}\boldsymbol{x}.$$

We also immediately get that

$$\lim_{m \to \infty} T_8^{(m)} = \int_0^T \varphi(t) \int_\Omega k_1(\boldsymbol{x}, s(\boldsymbol{x},t)) \Lambda(\boldsymbol{x}) (\nabla u(\boldsymbol{x},t) + \boldsymbol{g}_1) \cdot \nabla w(\boldsymbol{x}) \mathrm{d}\boldsymbol{x} \mathrm{d}t,$$

and

$$\lim_{m \to \infty} T_9^{(m)} = \int_0^T \varphi(t) \int_\Omega f_1(\boldsymbol{x},t) w(\boldsymbol{x}) \mathrm{d}\boldsymbol{x} \mathrm{d}t.$$

Since the set $\mathcal{T} = \{\sum_{i=1}^q \varphi_i(t) w_i(\boldsymbol{x}) \,:\, q \in \mathbb{N}, \varphi_i \in C_c^\infty[0,T), w_i \in C_c^\infty(\Omega)\}$ is dense in $C_c^\infty(\Omega \times [0,T))$, and since this reasoning is available as well for the second equation, we conclude the proof of Theorem 3.7. □

4 Strong convergence of (u, v)

We first state a continuity result at $t = 0$.

Lemma 4.1 *Under Hypotheses* (4)*, let* (u, v) *be a solution of* (5) *on* $(0, T)$ *and let us define* $p = u - v$*. Let* $\widetilde{S}$ *be defined by* (17)*. Then, the following properties hold:* $S(\cdot, p) \in C^0([0, T]; L^2(\Omega))$ *and* $S(\boldsymbol{x}, p(\boldsymbol{x}, 0)) = S(\boldsymbol{x}, p_{\rm ini}(\boldsymbol{x}))$ *for a.e.* $\boldsymbol{x} \in \Omega$*, and*

$$\widetilde{L} := \liminf_{h\to 0} \frac{1}{h} \int_0^h \int_\Omega \Phi(\boldsymbol{x}) \widetilde{S}(\boldsymbol{x}, p(\boldsymbol{x}, t)) \mathrm{d}\boldsymbol{x}\mathrm{d}t \geq \int_\Omega \Phi(\boldsymbol{x}) \widetilde{S}(\boldsymbol{x}, p_{\rm ini}(\boldsymbol{x}))\mathrm{d}\boldsymbol{x}. \tag{23}$$

Proof Let $j \in J$ be given, and, for all $\varepsilon > 0$, let $\psi_j^{(\varepsilon)} \in C_c^\infty(\Omega_j, [0, 1])$ be such that the measure of the set $\{\boldsymbol{x} \in \Omega_j,\ \psi_j^{(\varepsilon)}(\boldsymbol{x}) < 1\}$ is lower that ε. Let us consider the function $s_j^{(\varepsilon)} : (\boldsymbol{x}, t) \mapsto \psi_j^{(\varepsilon)}(\boldsymbol{x}) S_j(p(\boldsymbol{x}, t))$. Thanks to Hypotheses (4e) and to $u, v \in L^2(0, T; H_0^1(\Omega))$, we get that $s_j^{(\varepsilon)} \in L^2(0, T; H_0^1(\Omega_j))$. Introducing $\psi_j^{(\varepsilon)}$ as test function in (5) shows that $\Phi\partial_t s_j^{(\varepsilon)} \in L^2(0, T; H^{-1}(\Omega_j))$, and that we can write

$$\begin{aligned}
&\int_0^T \left(\langle \Phi \partial_t s_j^{(\varepsilon)}, w(t) \rangle_j + \int_\Omega k_1(S_j(p)) \Lambda(\boldsymbol{x}) (\nabla u + \boldsymbol{g}_1) \cdot (\psi_j^{(\varepsilon)} \nabla w + w \nabla \psi_j^{(\varepsilon)}) \mathrm{d}\boldsymbol{x} \right) \mathrm{d}t \\
&= \int_0^T \int_\Omega f_1 \psi_j^{(\varepsilon)} w \mathrm{d}\boldsymbol{x}\mathrm{d}t,\ \forall w \in L^2(0, T; H_0^1(\Omega_j)),
\end{aligned}$$

denoting by $\langle \cdot, \cdot \rangle_j$ the duality product $(H^{-1}(\Omega_j), H_0^1(\Omega_j))$. Considering the continuous embedding $T : L^2(\Omega_j) \to H^{-1}(\Omega_j)$, such that $T(u)(w) = \int_\Omega \Phi(\boldsymbol{x}) u(\boldsymbol{x}) w(\boldsymbol{x}) \mathrm{d}\boldsymbol{x}$ for all $u \in L^2(\Omega_j)$ and $w \in H_0^1(\Omega_j)$, this proves that $s_j^{(\varepsilon)} \in C^0([0, T], L^2(\Omega_j))$, and that

$$s_j^{(\varepsilon)}(\boldsymbol{x}, 0) = \psi_j^{(\varepsilon)}(\boldsymbol{x}) S_j(p_{\rm ini}(\boldsymbol{x})),\ \text{for a.e. } \boldsymbol{x} \in \Omega_j.$$

The inequality

$$\|S_j(p(\cdot, t)) - S_j(p(\cdot, s))\|^2_{L^2(\Omega_j)} \leq \varepsilon + \|\psi_j^{(\varepsilon)} S_j(p(\cdot, t)) - \psi_j^{(\varepsilon)} S_j(p(\cdot, s))\|^2_{L^2(\Omega_j)}$$

proves that $S_j(p(\cdot, \cdot)) \in C^0([0, T], L^2(\Omega_j))$, that

$$S_j(p(\cdot, 0)) = S_j(p_{\rm ini}(\boldsymbol{x})),\ \text{for a.e. } \boldsymbol{x} \in \Omega_j,$$

and that

$$\lim_{t\to 0} \|S_j(p(\cdot, t)) - S_j(p_{\rm ini})\|_{L^2(\Omega_j)} = 0.$$

These results yield $S(\cdot, p) \in C^0([0, T]; L^2(\Omega))$ and $S(\boldsymbol{x}, p(\boldsymbol{x}, 0)) = S(\boldsymbol{x}, p_{\rm ini}(\boldsymbol{x}))$ for a.e. $\boldsymbol{x} \in \Omega$.

Since the function S_j is nondecreasing its inverse function $S_j^{(-1)}$ is defined almost everywhere on $D_j := \bigcup_{A<B\in\mathbb{R}} [S_j(A), S_j(B)]$. We then denote

$$\gamma_j(s) = \int_{S_j(0)}^s S_j^{(-1)}(t)\mathrm{d}t,\ \forall s \in D_j.$$

Note that the function γ_j is nonnegative and continuous, and that

$$\widetilde{S}_j(q) = \gamma_j(S_j(q)),\ \forall q \in \mathbb{R}.$$

Since $S(\cdot, p) \in C^0([0, T]; L^2(\Omega))$ and $S(\boldsymbol{x}, p(\boldsymbol{x}, 0)) = S(\boldsymbol{x}, p_{\rm ini}(\boldsymbol{x}))$ for a.e. $\boldsymbol{x} \in \Omega$, we deduce by dominated convergence that for all $n \in \mathbb{N}$,

$$\lim_{h\to 0} \frac{1}{h} \int_0^h \int_\Omega \Phi(\boldsymbol{x}) \min(\widetilde{S}(\boldsymbol{x}, p(\boldsymbol{x}, t)), n) \mathrm{d}\boldsymbol{x}\mathrm{d}t = \int_\Omega \Phi(\boldsymbol{x}) \min(\widetilde{S}(\boldsymbol{x}, p_{\rm ini}(\boldsymbol{x})), n) \mathrm{d}\boldsymbol{x},$$

which shows that

$$\widetilde{L} \geq \int_\Omega \Phi(\boldsymbol{x}) \min(\widetilde{S}(\boldsymbol{x}, p_{\rm ini}(\boldsymbol{x})), n) \mathrm{d}\boldsymbol{x}, \quad \forall n \in \mathbb{N}.$$

By monotonous convergence, we get that

$$\widetilde{L} \geq \sup_{n\in\mathbb{N}} \int_\Omega \Phi(\boldsymbol{x}) \min(\widetilde{S}(\boldsymbol{x}, p_{\rm ini}(\boldsymbol{x})), n) \mathrm{d}\boldsymbol{x} = \int_\Omega \Phi(\boldsymbol{x}) \widetilde{S}(\boldsymbol{x}, p_{\rm ini}(\boldsymbol{x})) \mathrm{d}\boldsymbol{x},$$

which provides (23). □
We can now state the following property for solutions of (5).

Lemma 4.2 *Under Hypotheses* (4)*, let* (u, v) *be a solution of* (5) *on* $(0, T)$ *and let us define* $p = u - v$*. Let* $\widetilde{S}$ *be defined by* (17)*. Then the following property holds:*

$$\begin{aligned}
&\int_0^T \varphi'(t) \int_\Omega \Phi(\boldsymbol{x}) (S(\boldsymbol{x}, p(\boldsymbol{x}, t))(\bar{u} - \bar{v})(\boldsymbol{x}) - \widetilde{S}(\boldsymbol{x}, p(\boldsymbol{x}, t))) \mathrm{d}\boldsymbol{x}\mathrm{d}t \\
&+\varphi(0) \left(\int_\Omega \Phi(\boldsymbol{x}) (S(\boldsymbol{x}, p_{\rm ini}(\boldsymbol{x}))(\bar{u} - \bar{v})(\boldsymbol{x}) \mathrm{d}\boldsymbol{x} - \widetilde{L} \right) \\
&+ \int_0^T \varphi(t) \int_\Omega (k_1(S(p)) \Lambda(\nabla u + \boldsymbol{g}_1) \cdot \nabla(u - \bar{u}) + k_2(S(p)) \Lambda(\nabla v + \boldsymbol{g}_2) \cdot \nabla(v - \bar{v})) \, \mathrm{d}\boldsymbol{x}\mathrm{d}t \\
&= \int_0^T \varphi(t) \int_\Omega (f_1(u - \bar{u}) + f_2(v - \bar{v})) \mathrm{d}\boldsymbol{x}\mathrm{d}t, \ \forall \varphi \in C_c^\infty((-\infty, T)),
\end{aligned} \tag{24}$$

where $\widetilde{L}$*, defined in Lemma 4.1, satisfies* $\widetilde{L} = \lim_{h\to 0} \frac{1}{h} \int_0^h \int_\Omega \Phi(\boldsymbol{x}) \widetilde{S}(\boldsymbol{x}, p(\boldsymbol{x}, t)) \mathrm{d}\boldsymbol{x}\mathrm{d}t$ *(and not only "*$\liminf$*").*

Proof Let $w \in C_c^\infty(\Omega \times (-\infty, T))$ and $h \in (0, T)$ such that $w(\cdot, t) = 0$ for $t \in [T - h, T]$ be given. Let us consider, in (5), the test function $(\boldsymbol{x}, t) \mapsto \frac{1}{h} \int_{t-h}^t w(\boldsymbol{x}, s) \mathrm{d}s$, which belongs to $C_c^\infty(\Omega \times [0, T))$. We obtain that

$$\begin{aligned}
&- \int_0^T \int_\Omega \Phi(\boldsymbol{x}) S(\boldsymbol{x}, p(\boldsymbol{x}, t)) \partial_t \left(\frac{1}{h} \int_{t-h}^t w(\boldsymbol{x}, s) \right) \mathrm{d}s\mathrm{d}\boldsymbol{x}\mathrm{d}t - \int_\Omega \Phi(\boldsymbol{x}) S(\boldsymbol{x}, p_{\rm ini}(\boldsymbol{x})) \frac{1}{h} \int_{-h}^0 w(\boldsymbol{x}, s) \mathrm{d}s\mathrm{d}\boldsymbol{x} \\
&= \int_0^T \frac{1}{h} \int_{t-h}^t \int_\Omega (f_1(\boldsymbol{x}, t) w(\boldsymbol{x}, s) - k_1(\boldsymbol{x}, S(\boldsymbol{x}, p(\boldsymbol{x}, t))) \Lambda(\boldsymbol{x}) (\nabla u(\boldsymbol{x}, t) + \boldsymbol{g}_1) \cdot \nabla w(\boldsymbol{x}, s)) \mathrm{d}\boldsymbol{x}\mathrm{d}s\mathrm{d}t,
\end{aligned}$$

and a similar second equation. This provides, using $w(\cdot, t) = 0$ for $t \in [T - h, T]$,

$$\begin{aligned}
&\frac{1}{h} \int_0^T \int_\Omega \Phi(\boldsymbol{x}) (S(\boldsymbol{x}, p(\boldsymbol{x}, t + h)) - S(\boldsymbol{x}, p(\boldsymbol{x}, t))) w(\boldsymbol{x}, t) \mathrm{d}\boldsymbol{x}\mathrm{d}t \\
&- \int_\Omega \Phi(\boldsymbol{x}) \frac{1}{h} \int_{-h}^0 (S(\boldsymbol{x}, p_{\rm ini}(\boldsymbol{x})) - S(\boldsymbol{x}, p(\boldsymbol{x}, s + h))) w(\boldsymbol{x}, s) \mathrm{d}s\mathrm{d}\boldsymbol{x} \\
&= \int_0^T \frac{1}{h} \int_{t-h}^t \int_\Omega (f_1(\boldsymbol{x}, t) w(\boldsymbol{x}, s) - k_1(\boldsymbol{x}, S(\boldsymbol{x}, p(\boldsymbol{x}, t))) \Lambda(\boldsymbol{x}) (\nabla u(\boldsymbol{x}, t) + \boldsymbol{g}_1) \cdot \nabla w(\boldsymbol{x}, s)) \mathrm{d}\boldsymbol{x}\mathrm{d}s\mathrm{d}t,
\end{aligned} \tag{25}$$

and a similar second equation.

Let $\varphi \in C_c^\infty((-\infty, T), \mathbb{R}^+)$ be given, and let us define $u(\cdot, t) = \bar{u}$ for a.e. $t < 0$. Considering $h \in (0, T)$ such that $\varphi(t) = 0$ for $t \in [T - h, T]$, we can approximate $(u - \bar{u})\varphi \in L^2(-h, T; H_0^1(\Omega))$ by functions $w \in C_c^\infty(\Omega \times (-\infty, T))$ such that $w(\cdot, t) = 0$ for any $t \in [T - h, T]$. Hence, letting $w \to (u - \bar{u})\varphi$ and $\nabla w \to \nabla(u - \bar{u})\varphi$ in (25), we obtain

$$\begin{aligned}
&\frac{1}{h} \int_0^T \int_\Omega \Phi(\boldsymbol{x}) (S(\boldsymbol{x}, p(\boldsymbol{x}, t + h)) - S(\boldsymbol{x}, p(\boldsymbol{x}, t))) (u(\boldsymbol{x}, t) - \bar{u}(\boldsymbol{x})) \varphi(t) \mathrm{d}\boldsymbol{x}\mathrm{d}t \\
= \int_0^T \frac{1}{h} \int_{t-h}^t \int_\Omega (\quad & f_1(\boldsymbol{x}, t)(u(\boldsymbol{x}, s) - \bar{u}(\boldsymbol{x}))\varphi(s) \\
& - k_1(\boldsymbol{x}, S(\boldsymbol{x}, p(\boldsymbol{x}, t))) \Lambda(\boldsymbol{x}) (\nabla u(\boldsymbol{x}, t) + \boldsymbol{g}_1) \cdot (\nabla u(\boldsymbol{x}, s) - \nabla \bar{u}(\boldsymbol{x})) \varphi(s)) \mathrm{d}\boldsymbol{x}\mathrm{d}s\mathrm{d}t.
\end{aligned}$$

We now define $v(\cdot,t)=\bar{v}$ for a.e. $t<0$. Since $(v-\bar{v})\varphi \in L^2(-h,T;H_0^1(\Omega))$, we can similarly let $w \to (v-\bar{v})\varphi$ in the second equation, which provides

$$\begin{aligned}
&-\frac{1}{h}\int_0^T\int_\Omega \Phi(\boldsymbol{x})(S(\boldsymbol{x},p(\boldsymbol{x},t+h))-S(\boldsymbol{x},p(\boldsymbol{x},t)))(v(\boldsymbol{x},t)-\bar{v}(\boldsymbol{x}))\varphi(t)\mathrm{d}\boldsymbol{x}\mathrm{d}t\\
=&\int_0^T\frac{1}{h}\int_{t-h}^t\int_\Omega\Big(\quad f_2(\boldsymbol{x},t)(v(\boldsymbol{x},s)-\bar{v}(\boldsymbol{x}))\varphi(s)\\
&\qquad -k_2(\boldsymbol{x},S(\boldsymbol{x},p(\boldsymbol{x},t)))\Lambda(\boldsymbol{x})(\nabla v(\boldsymbol{x},t)+\boldsymbol{g}_2)\cdot(\nabla v(\boldsymbol{x},s)-\nabla\bar{v}(\boldsymbol{x}))\varphi(s))\mathrm{d}\boldsymbol{x}\mathrm{d}s\mathrm{d}t.
\end{aligned}$$

We then add the two above equations. We get $T_{10}(h)=T_{11}(h)$ with

$$T_{10}(h)=\frac{1}{h}\int_0^T\int_\Omega \Phi(\boldsymbol{x})(S(\boldsymbol{x},p(\boldsymbol{x},t+h))-S(\boldsymbol{x},p(\boldsymbol{x},t)))(p(\boldsymbol{x},t)-(\bar{u}-\bar{v})(\boldsymbol{x}))\varphi(t)\mathrm{d}\boldsymbol{x}\mathrm{d}t,$$

and

$$\begin{aligned}
&T_{11}(h)\\
&=\int_0^T\frac{1}{h}\int_{t-h}^t\int_\Omega\Big(\quad f_1(\boldsymbol{x},t)(u(\boldsymbol{x},s)-\bar{u}(\boldsymbol{x}))\varphi(s)\\
&\qquad -k_1(\boldsymbol{x},S(\boldsymbol{x},p(\boldsymbol{x},t)))\Lambda(\boldsymbol{x})(\nabla u(\boldsymbol{x},t)+\boldsymbol{g}_1)\cdot(\nabla u(\boldsymbol{x},s)-\nabla\bar{u}(\boldsymbol{x}))\varphi(s))\mathrm{d}\boldsymbol{x}\mathrm{d}s\mathrm{d}t\\
&+\int_0^T\frac{1}{h}\int_{t-h}^t\int_\Omega\Big(\quad f_2(\boldsymbol{x},t)(v(\boldsymbol{x},s)-\bar{v}(\boldsymbol{x}))\varphi(s)\\
&\qquad -k_2(\boldsymbol{x},S(\boldsymbol{x},p(\boldsymbol{x},t)))\Lambda(\boldsymbol{x})(\nabla v(\boldsymbol{x},t)+\boldsymbol{g}_2)\cdot(\nabla v(\boldsymbol{x},s)-\nabla\bar{v}(\boldsymbol{x}))\varphi(s))\mathrm{d}\boldsymbol{x}\mathrm{d}s\mathrm{d}t.
\end{aligned}$$

Observing that $\int_a^b qS_j'(q)\mathrm{d}q=\widetilde{S}_j(b)-\widetilde{S}_j(a)=a(S_j(b)-S_j(a))+\int_a^b(S_j(b)-S_j(q))\mathrm{d}q$ which implies $\widetilde{S}_j(b)-\widetilde{S}_j(a)\geq a(S_j(b)-S_j(a))$, we get that $T_{10}(h)\leq T_{12}(h)$ with

$$\begin{aligned}
T_{12}(h)=\frac{1}{h}\int_0^T\int_\Omega\Phi(\boldsymbol{x})\Big(\quad &(\widetilde{S}(\boldsymbol{x},p(\boldsymbol{x},t+h))-\widetilde{S}(\boldsymbol{x},p(\boldsymbol{x},t)))\\
&-(S(\boldsymbol{x},p(\boldsymbol{x},t+h))-S(\boldsymbol{x},p(\boldsymbol{x},t)))(\bar{u}-\bar{v})(\boldsymbol{x})\Big)\varphi(t)\mathrm{d}\boldsymbol{x}\mathrm{d}t,
\end{aligned}$$

which can be rewritten as

$$\begin{aligned}
T_{12}(h)=&-\int_0^T\int_\Omega\Phi(\boldsymbol{x})(\widetilde{S}(\boldsymbol{x},p(\boldsymbol{x},t))-S(\boldsymbol{x},p(\boldsymbol{x},t)))(\bar{u}-\bar{v})(\boldsymbol{x}))\frac{1}{h}(\varphi(t)-\varphi(t-h))\mathrm{d}\boldsymbol{x}\mathrm{d}t\\
&-\frac{1}{h}\int_{-h}^0\int_\Omega\Phi(\boldsymbol{x})(\widetilde{S}(\boldsymbol{x},p(\boldsymbol{x},t+h))-S(\boldsymbol{x},p(\boldsymbol{x},t+h)))(\bar{u}-\bar{v})(\boldsymbol{x}))\varphi(t)\mathrm{d}\boldsymbol{x}\mathrm{d}t,
\end{aligned}$$

hence leading to $T_{12}(h)\geq T_{11}(h)$. Now letting $w\to(u(\cdot,t+h)-\bar{u})\varphi$ in (25) and $w\to(v(\cdot,t+h)-\bar{v})\varphi$ in the second similar equation to (25), adding the result, we get $T_{13}(h)-T_{14}(h)=T_{15}(h)$ with

$$T_{13}(h)=\frac{1}{h}\int_0^T\int_\Omega\Phi(\boldsymbol{x})(S(\boldsymbol{x},p(\boldsymbol{x},t+h))-S(\boldsymbol{x},p(\boldsymbol{x},t)))(p(\boldsymbol{x},t+h)-(\bar{u}-\bar{v})(\boldsymbol{x}))\varphi(t)\mathrm{d}\boldsymbol{x}\mathrm{d}t,$$

$$T_{14}(h)=\int_\Omega\Phi(\boldsymbol{x})\frac{1}{h}\int_{-h}^0(S(\boldsymbol{x},p_{\mathrm{ini}}(\boldsymbol{x}))-S(\boldsymbol{x},p(\boldsymbol{x},s+h)))(p(\boldsymbol{x},s+h)-(\bar{u}-\bar{v})(\boldsymbol{x}))\varphi(s)\mathrm{d}s\mathrm{d}\boldsymbol{x},$$

and

$$\begin{aligned}
&T_{15}(h)=\\
&\int_0^T\frac{1}{h}\int_{t-h}^t\int_\Omega\Big(\quad f_1(\boldsymbol{x},t)(u(\boldsymbol{x},s+h)-\bar{u}(\boldsymbol{x}))\varphi(s)\\
&\qquad -k_1(\boldsymbol{x},S(\boldsymbol{x},p(\boldsymbol{x},t)))\Lambda(\boldsymbol{x})(\nabla u(\boldsymbol{x},t)+\boldsymbol{g}_1)\cdot(\nabla u(\boldsymbol{x},s+h)-\nabla\bar{u}(\boldsymbol{x}))\varphi(s))\mathrm{d}\boldsymbol{x}\mathrm{d}s\mathrm{d}t\\
&+\int_0^T\frac{1}{h}\int_{t-h}^t\int_\Omega\Big(\quad f_2(\boldsymbol{x},t)(v(\boldsymbol{x},s+h)-\bar{v}(\boldsymbol{x}))\varphi(s)\\
&\qquad -k_2(\boldsymbol{x},S(\boldsymbol{x},p(\boldsymbol{x},t)))\Lambda(\boldsymbol{x})(\nabla v(\boldsymbol{x},t)+\boldsymbol{g}_2)\cdot(\nabla v(\boldsymbol{x},s+h)-\nabla\bar{v}(\boldsymbol{x}))\varphi(s))\mathrm{d}\boldsymbol{x}\mathrm{d}s\mathrm{d}t.
\end{aligned}$$

Now using the inequality $\int_a^b qS_j'(q)\mathrm{d}q = \widetilde{S}_j(b) - \widetilde{S}_j(a) = b(S_j(b) - S_j(a)) - \int_a^b (S_j(q) - S_j(a))\mathrm{d}q$, we get $T_{13}(h) \geq T_{12}(h)$ and therefore $T_{12}(h) \leq T_{15}(h) + T_{14}(h)$. Moreover, defining $T_{16}(h)$ by

$$T_{16}(h) = \int_\Omega \Phi(\boldsymbol{x}) \frac{1}{h} \int_{-h}^0 (S(\boldsymbol{x}, p_{\mathrm{ini}}(\boldsymbol{x})) - S(\boldsymbol{x}, p(\boldsymbol{x}, s+h))(p_{\mathrm{ini}}(\boldsymbol{x}) - (\bar{u} - \bar{v})(\boldsymbol{x}))\varphi(s)\mathrm{d}s\mathrm{d}\boldsymbol{x},$$

we have

$$T_{14}(h) = T_{16}(h) - \int_\Omega \Phi(\boldsymbol{x}) \frac{1}{h} \int_{-h}^0 (S(\boldsymbol{x}, p_{\mathrm{ini}}(\boldsymbol{x})) - S(\boldsymbol{x}, p(\boldsymbol{x}, s+h))(p_{\mathrm{ini}}(\boldsymbol{x}) - p(\boldsymbol{x}, s+h))\varphi(s)\mathrm{d}s\mathrm{d}\boldsymbol{x},$$

which implies $T_{14}(h) \leq T_{16}(h)$. Gathering the results, we get

$$T_{11}(h) \leq T_{12}(h) \leq T_{15}(h) + T_{16}(h). \tag{26}$$

Let us remark that, defining T_{17} by

$$T_{17} = \int_0^T \varphi \int_\Omega \Big(\begin{array}{l} (f_1(u-\bar{u}) + f_2(v-\bar{v})) - \\ (k_1(\cdot, S(p))\Lambda(\nabla u + \boldsymbol{g}_1)\cdot\nabla(u-\bar{u}) + k_2(\cdot, S(p))\Lambda(\nabla v + \boldsymbol{g}_2)\cdot\nabla(v-\bar{v}))\Big)\mathrm{d}\boldsymbol{x}\mathrm{d}t, \end{array}$$

we get that

$$\lim_{h\to 0} T_{11}(h) = \lim_{h\to 0} T_{15}(h) = T_{17}.$$

Using Lemma (4.1) and the regularity of φ, we get that

$$\lim_{h\to 0} T_{16}(h) = 0.$$

Hence we get, passing to the limit in (26), that

$$\lim_{h\to 0} T_{12}(h) = T_{17}.$$

Since

$$\begin{aligned} &\lim_{h\to 0} \int_0^T \int_\Omega \Phi(\boldsymbol{x})(\widetilde{S}(\boldsymbol{x}, p(\boldsymbol{x}, t)) - S(\boldsymbol{x}, p(\boldsymbol{x}, t))(\bar{u} - \bar{v})(\boldsymbol{x})) \frac{1}{h}(\varphi(t) - \varphi(t-h))\mathrm{d}\boldsymbol{x}\mathrm{d}t \\ &= \int_0^T \int_\Omega \Phi(\boldsymbol{x})(\widetilde{S}(\boldsymbol{x}, p(\boldsymbol{x}, t)) - S(\boldsymbol{x}, p(\boldsymbol{x}, t))(\bar{u} - \bar{v})(\boldsymbol{x}))\varphi'(t)\mathrm{d}\boldsymbol{x}\mathrm{d}t \end{aligned}$$

and

$$\begin{aligned} &\lim_{h\to 0} \frac{1}{h} \int_{-h}^0 \int_\Omega \Phi(\boldsymbol{x}) S(\boldsymbol{x}, p(\boldsymbol{x}, t+h))(\bar{u} - \bar{v})(\boldsymbol{x})\varphi(t)\mathrm{d}\boldsymbol{x}\mathrm{d}t \\ &= \int_\Omega \Phi(\boldsymbol{x}) S(\boldsymbol{x}, p_{\mathrm{ini}}(\boldsymbol{x}))(\bar{u} - \bar{v})(\boldsymbol{x})\varphi(0)\mathrm{d}\boldsymbol{x}, \end{aligned}$$

we get that

$$\lim_{h\to 0} \frac{1}{h} \int_{-h}^0 \int_\Omega \Phi(\boldsymbol{x}) \widetilde{S}(\boldsymbol{x}, p(\boldsymbol{x}, t+h))\varphi(t)\mathrm{d}\boldsymbol{x}\mathrm{d}t = \varphi(0)\widetilde{L}.$$

Gathering the above results, we get that (24) holds for $\varphi \in C_c^\infty((-\infty, T), \mathbb{R}^+)$. Writing $\varphi = \max(\varphi, 0) - \max(-\varphi, 0)$ and taking regularizations, we conclude (24) for all $\varphi \in C^\infty((-\infty, T))$.
□

Let us now state a discrete property.

Lemma 4.3 *Under Hypotheses* (4)*, let $\mathcal{D}$ be a space-time gradient discretisation in the sense of Definition 2.8. Let u, v be such that Scheme* (14)*, $p = u - v$ and let $\varphi_{\mathcal{D}}$ be the function equal to $\varphi(t^{(n)})$ on the interval $(t^{(n)}, t^{(n+1)})$, for all $n = 0, \dots, N-1$; then*

$$\begin{aligned}\int_0^T \varphi'(t) \int_\Omega \Phi(\boldsymbol{x}) \left(S(\boldsymbol{x}, \Pi_{\mathcal{D}} p(\boldsymbol{x}, t)) \Pi_{\mathcal{D}}(\bar{u}_{\mathcal{D}} - \bar{v}_{\mathcal{D}})(\boldsymbol{x}) - \widetilde{S}(\boldsymbol{x}, \Pi_{\mathcal{D}} p(\boldsymbol{x}, t)) \right) \mathrm{d}\boldsymbol{x}\mathrm{d}t \\ + \varphi(0) \int_\Omega \Phi(\boldsymbol{x}) \left(S(\boldsymbol{x}, \Pi_{\mathcal{D}} p^{(0)}(\boldsymbol{x})) \Pi_{\mathcal{D}}(\bar{u}_{\mathcal{D}} - \bar{v}_{\mathcal{D}})(\boldsymbol{x}) - \widetilde{S}(\boldsymbol{x}, \Pi_{\mathcal{D}} p^{(0)}(\boldsymbol{x})) \right) \mathrm{d}\boldsymbol{x} \\ + \int_0^T \varphi_{\mathcal{D}}(t) \int_\Omega (k_1(S(\Pi_{\mathcal{D}} p)) \Lambda(\nabla_{\mathcal{D}} u + \boldsymbol{g}_1) \cdot \nabla_{\mathcal{D}}(u - \bar{u}_{\mathcal{D}}) + k_2(S(\Pi_{\mathcal{D}} p)) \Lambda(\nabla_{\mathcal{D}} v + \boldsymbol{g}_2) \cdot \nabla_{\mathcal{D}}(v - \bar{v}_{\mathcal{D}})) \, \mathrm{d}\boldsymbol{x}\mathrm{d}t \\ \leq \int_0^T \varphi_{\mathcal{D}}(t) \int_\Omega (f_1 \Pi_{\mathcal{D}}(u - \bar{u}_{\mathcal{D}}) + f_2 \Pi_{\mathcal{D}}(v - \bar{v}_{\mathcal{D}})) \mathrm{d}\boldsymbol{x}\mathrm{d}t, \ \forall \varphi \in C_c^\infty([0,T), \mathbb{R}^+). \quad (27)\end{aligned}$$

Proof As in the proof of Lemma 3.2, we introduce $w = \delta t^{(n+\frac{1}{2})}(u^{(n+1)} - \bar{u}_{\mathcal{D}})\varphi(t^{(n)})$ and $\delta t^{(n+\frac{1}{2})}(v^{(n+1)} - \bar{v}_{\mathcal{D}})\varphi(t^{(n)})$ as test functions in Scheme (14), and we use the same inequality concerning $\widetilde{S}$. □
We may now state the strong convergence of the scheme.

Theorem 4.4 (Strong convergence of the numerical scheme) *Under the assumptions of Theorem 3.7, there exist $u, v \in (L^2(\Omega \times (0,T)))^2$ and $p = u - v$ such that, for any $t_0 \in (0,T)$, up to a subsequence,*

1. *$(\Pi_{\mathcal{D}_m} u_m, \Pi_{\mathcal{D}_m} v_m)$ converges in $L^2(\Omega \times (0,t_0))^2$ to (u,v) as $m \to \infty$,*
2. *$(\nabla_{\mathcal{D}_m} u_m, \nabla_{\mathcal{D}_m} v_m)$ converges in $(L^2(\Omega \times (0,t_0))^d)^2$ to $(\nabla u, \nabla v)$ as $m \to \infty$,*
3. *$s_{\mathcal{D}_m}$ converges in $L^2(\Omega \times (0,T))$ to s such that $s(\boldsymbol{x},t) = S(\boldsymbol{x}, p(\boldsymbol{x},t))$, for a.e. $(\boldsymbol{x},t) \in \Omega \times (0,T)$ as $m \to \infty$,*

and (u,v) is a weak solution of Problem (5)*.*

Proof We first apply Theorem 3.7, which shows the weak convergence properties for $(\Pi_{\mathcal{D}_m} u_m, \Pi_{\mathcal{D}_m} v_m)$, and the strong one for $s_{\mathcal{D}_m}$. Since we have

$$\begin{aligned}|\widetilde{S}_j(a) - \widetilde{S}_j(b)| = \left| \int_a^b q S_j'(q) \mathrm{d}q \right| \leq \left(\int_a^b S_j'(q) \mathrm{d}q \int_a^b q^2 S_j'(q) \mathrm{d}q \right)^{1/2} \\ \leq \left(L_S |S_j(b) - S_j(a)| |b^3 - a^3|/3 \right)^{1/2},\end{aligned}$$

we have, thanks to the Young inequality, for $p, q \in L^2(\Omega)$,

$$\begin{aligned}\int_\Omega |\widetilde{S}(\boldsymbol{x}, p(\boldsymbol{x})) - \widetilde{S}(\boldsymbol{x}, q(\boldsymbol{x}))| \mathrm{d}\boldsymbol{x} \leq \ & \left(\int_\Omega |S(\boldsymbol{x}, p(\boldsymbol{x})) - S(\boldsymbol{x}, q(\boldsymbol{x}))|^2 \mathrm{d}\boldsymbol{x} \right)^{1/4} \\ & \times \left(\int_\Omega \left(\frac{L_S}{3} |p(\boldsymbol{x})^3 - q(\boldsymbol{x})^3| \right)^{2/3} \mathrm{d}\boldsymbol{x} \right)^{3/4}. \quad (28)\end{aligned}$$

Therefore, we may write

$$\lim_{m \to \infty} \int_0^T \int_\Omega |\widetilde{S}(\boldsymbol{x}, \Pi_{\mathcal{D}_m} p_m(\boldsymbol{x},t)) - \widetilde{S}(\boldsymbol{x}, p(\boldsymbol{x},t))| \mathrm{d}\boldsymbol{x}\mathrm{d}t = 0,$$

and

$$\lim_{m \to \infty} \int_\Omega |\widetilde{S}(\boldsymbol{x}, \Pi_{\mathcal{D}_m} p_m^{(0)}(\boldsymbol{x})) - \widetilde{S}(\boldsymbol{x}, p_{\mathrm{ini}}(\boldsymbol{x}))| \mathrm{d}\boldsymbol{x} = 0.$$

Passing to the limit sup as $m \to \infty$ in (27) and subtract (24). We thus obtain, defining $\varphi_{\mathcal{D}_m}(t)$ as in the statement of Lemma 4.3,

$$
\begin{aligned}
&- \varphi(0) \int_\Omega \Phi(\boldsymbol{x}) \widetilde{S}(\boldsymbol{x}, p_{\rm ini}(\boldsymbol{x})) \mathrm{d}\boldsymbol{x} \\
&+ \limsup_{m\to\infty} \int_0^T \varphi_{\mathcal{D}_m}(t) \int_\Omega (k_1(S(\Pi_{\mathcal{D}_m} p_m))\Lambda \nabla_{\mathcal{D}_m} u_m \cdot \nabla_{\mathcal{D}_m} u_m + k_2(S(\Pi_{\mathcal{D}_m} p_m))\Lambda \nabla_{\mathcal{D}_m} v_m \cdot \nabla_{\mathcal{D}_m} v_m) \, \mathrm{d}\boldsymbol{x}\mathrm{d}t \\
&\qquad \le -\varphi(0)\widetilde{L} + \int_0^T \varphi(t) \int_\Omega (k_1(S(p))\Lambda \nabla u \cdot \nabla u + k_2(S(p))\Lambda \nabla v \cdot \nabla v) \, \mathrm{d}\boldsymbol{x}\mathrm{d}t.
\end{aligned}
$$

Using (23), we obtain

$$
\begin{aligned}
&\limsup_{m\to\infty} \int_0^T \varphi_{\mathcal{D}_m}(t) \int_\Omega (k_1(S(\Pi_{\mathcal{D}_m} p_m))\Lambda \nabla_{\mathcal{D}_m} u_m \cdot \nabla_{\mathcal{D}_m} u_m + k_2(S(\Pi_{\mathcal{D}_m} p_m))\Lambda \nabla_{\mathcal{D}_m} v_m \cdot \nabla_{\mathcal{D}_m} v_m) \, \mathrm{d}\boldsymbol{x}\mathrm{d}t \\
&\qquad \le \int_0^T \varphi(t) \int_\Omega (k_1(S(p))\Lambda \nabla u \cdot \nabla u + k_2(S(p))\Lambda \nabla v \cdot \nabla v) \, \mathrm{d}\boldsymbol{x}\mathrm{d}t.
\end{aligned}
$$

On the other hand, standard properties for weak convergence show that

$$
\begin{aligned}
&\liminf_{m\to\infty} \int_0^T \varphi_{\mathcal{D}_m}(t) \int_\Omega (k_1(S(\Pi_{\mathcal{D}_m} p_m))\Lambda \nabla_{\mathcal{D}_m} u_m \cdot \nabla_{\mathcal{D}_m} u_m + k_2(S(\Pi_{\mathcal{D}_m} p_m))\Lambda \nabla_{\mathcal{D}_m} v_m \cdot \nabla_{\mathcal{D}_m} v_m) \, \mathrm{d}\boldsymbol{x}\mathrm{d}t \\
&\qquad \ge \int_0^T \varphi(t) \int_\Omega (k_1(S(p))\Lambda \nabla u \cdot \nabla u + k_2(S(p))\Lambda \nabla v \cdot \nabla v) \, \mathrm{d}\boldsymbol{x}\mathrm{d}t,
\end{aligned}
$$

which proves that

$$
\begin{aligned}
&\lim_{m\to\infty} \int_0^T \varphi_{\mathcal{D}_m}(t) \int_\Omega (k_1(S(\Pi_{\mathcal{D}_m} p_m))\Lambda \nabla_{\mathcal{D}_m} u_m \cdot \nabla_{\mathcal{D}_m} u_m + k_2(S(\Pi_{\mathcal{D}_m} p_m))\Lambda \nabla_{\mathcal{D}_m} v_m \cdot \nabla_{\mathcal{D}_m} v_m) \, \mathrm{d}\boldsymbol{x}\mathrm{d}t \\
&\qquad = \int_0^T \varphi(t) \int_\Omega (k_1(S(p))\Lambda \nabla u \cdot \nabla u + k_2(S(p))\Lambda \nabla v \cdot \nabla v) \, \mathrm{d}\boldsymbol{x}\mathrm{d}t.
\end{aligned}
$$

We then get that

$$
\begin{aligned}
\lim_{m\to\infty} \int_0^T \varphi_{\mathcal{D}_m}(t) \int_\Omega \Big(& k_1(S(\Pi_{\mathcal{D}_m} p_m))\Lambda (\nabla_{\mathcal{D}_m} u_m - \nabla u) \cdot (\nabla_{\mathcal{D}_m} u_m - \nabla u) \\
& + k_2(S(\Pi_{\mathcal{D}_m} p_m))\Lambda (\nabla_{\mathcal{D}_m} v_m - \nabla v) \cdot (\nabla_{\mathcal{D}_m} v_m - \nabla v) \Big) \mathrm{d}\boldsymbol{x}\mathrm{d}t = 0.
\end{aligned}
$$

Taking $\varphi(t) = 1$ on $[0, t_0]$ for any $t_0 \in (0, T)$, this concludes the proof of the convergence in $L^2(\Omega \times (0, t_0))$ of the approximate gradients. Let us show that this implies the convergence of the approximate solutions $(\Pi_{\mathcal{D}_m} u_m, \Pi_{\mathcal{D}_m} v_m)$. For a.e. $t \in (0, t_0)$, let $\widehat{u}_m(t)$ be defined by

$$
\widehat{u}_m(t) = \operatorname*{argmin}_{z \in X_{\mathcal{D}_m,0}} \left(\|\Pi_{\mathcal{D}_m} z - (u(t) - \bar{u})\|_{L^2(\Omega)} + \|\nabla_{\mathcal{D}_m} z - \nabla(u(t) - \bar{u})\|_{L^2(\Omega)^d} \right).
$$

We get, using

$$
\|\Pi_{\mathcal{D}_m} \widehat{u}_m(t) - (u(t) - \bar{u})\|_{L^2(\Omega)} + \|\nabla_{\mathcal{D}_m} \widehat{u}_m(t) - \nabla(u(t) - \bar{u})\|_{L^2(\Omega)^d} \le \|u(t) - \bar{u}\|_{L^2(\Omega)} + \|\nabla(u(t) - \bar{u})\|_{L^2(\Omega)^d}
$$

(since $0 \in X_{\mathcal{D}_m,0}$) that $\int_0^T \|\Pi_{\mathcal{D}_m}\widehat{u}_m(t) - (u(t)-\bar{u})\|^2_{L^2(\Omega)}\mathrm{d}t$ and $\int_0^T \|\nabla_{\mathcal{D}_m}\widehat{u}_m(t) - \nabla(u(t)-\bar{u})\|^2_{L^2(\Omega)^d}\mathrm{d}t$ tend to 0 by dominated convergence. We then have, thanks to the coercivity hypothesis,

$$\|\Pi_{\mathcal{D}_m}(u_m - \bar{u}_{\mathcal{D}} - \widehat{u}_m)\|_{L^2(\Omega\times(0,t_0))} \le C_P\|\nabla_{\mathcal{D}_m}(u_m - \bar{u}_{\mathcal{D}} - \widehat{u}_m)\|_{L^2(\Omega\times(0,t_0))^d}.$$

We thus get, thanks to the triangle inequality that

$$\|\Pi_{\mathcal{D}_m}u_m - u\|_{L^2(\Omega\times(0,t_0))} \le \|u - \Pi_{\mathcal{D}_m}(\bar{u}_{\mathcal{D}_m} + \widehat{u}_m)\|_{L^2(\Omega\times(0,t_0))} + C_P\|\nabla_{\mathcal{D}_m}(u_m - \bar{u}_{\mathcal{D}_m} - \widehat{u}_m)\|_{L^2(\Omega\times(0,t_0))^d},$$

which implies, thanks again to the triangle inequality,

$$\begin{aligned}&\|\Pi_{\mathcal{D}_m}u_m - u\|_{L^2(\Omega\times(0,t_0))} \le \|u - \Pi_{\mathcal{D}_m}(\bar{u}_{\mathcal{D}_m} + \widehat{u}_m)\|_{L^2(\Omega\times(0,t_0))}\\ &+C_P(\|\nabla_{\mathcal{D}_m}u_m - \nabla u\|_{L^2(\Omega\times(0,t_0))^d} + \|\nabla u - \nabla_{\mathcal{D}_m}(\bar{u}_{\mathcal{D}_m} + \widehat{u}_m)\|_{L^2(\Omega\times(0,t_0))^d}).\end{aligned}$$

We then get

$$\lim_{m\to\infty}\|\Pi_{\mathcal{D}_m}u_m - u\|_{L^2(\Omega\times(0,t_0))} = 0.$$

The same arguments apply for v, and concludes the proof. □

5 Numerical examples

In the numerical tests proposed in this section, we use the Vertex Approximate Gradient scheme, denoted VAG, introduced in [17] and developed for compositional multiphase flows in porous media in [18]. Following the gradient scheme framework, we first recall the construction of the VAG scheme, then we present several numerical experiments which are focused on the simulation of oil migration in a basin with discontinuous capillary pressures. Such problems are widely used in petroleum engineering for basin modeling in order to simulate oil trapping. The aim of this section is first to validate the scheme presented previously, by comparison with a classical upwind approximation of the mobility terms widely used in the oil industry. More precisely, we compare the centered approximation of the relative permeabilities corresponding to our scheme (14), with an upwind first order approximation of the relative permeability of each phase with respect to the sign of the phase Darcy flux (see [3, 22], and [18] in the framework of the VAG scheme). A second objective is to assess the hypothesis (4g) by comparison of the results obtained with $k_{\min} > 0$ with those obtained in the limit case $k_{\min} = 0$ which matches the physical model.

5.1 The Vertex Approximate Gradient scheme

In the VAG scheme, a primary polyhedral mesh $\mathcal{M}$ is given. We assume that each element $K \in \mathcal{M}$ is strictly star-shaped with respect to some point $\boldsymbol{x}_K$. We denote by $\mathcal{E}_K$ the set of all interfaces $\overline{K}\cap\overline{L}$, for all neighbors of K denoted by $L \in \mathcal{M}$ and, for a boundary control volume, $\mathcal{E}_K$ also contains the element $\overline{K}\cap\partial\Omega$. Each $\sigma \in \mathcal{E}_K$ is assumed to be the reunion of $d-1$ simplices (segments if $d=2$, triangles if $d=3$) denoted $\tau \in \mathcal{S}_\sigma$. We denote by $\mathcal{V}_\sigma$ the set of all the vertices of σ, located at the boundary of σ, and by $\mathcal{V}_\sigma^0$ the set of all the internal vertices of σ. We assume that, for all $\boldsymbol{v} \in \mathcal{V}_\sigma^0$, there exist some coefficients $(\alpha_{\boldsymbol{v}}^{\boldsymbol{x}})_{\boldsymbol{x}\in\mathcal{V}_\sigma}$, such that

$$\boldsymbol{v} = \sum_{\boldsymbol{x}\in\mathcal{V}_\sigma}\alpha_{\boldsymbol{v}}^{\boldsymbol{x}}\boldsymbol{x}, \text{ with } \sum_{\boldsymbol{x}\in\mathcal{V}_\sigma}\alpha_{\boldsymbol{v}}^{\boldsymbol{x}} = 1.$$

Therefore, if $d=2$ we can simply take $\mathcal{V}_\sigma^0 = \emptyset$ and the d vertices of any $\tau \in \mathcal{S}_\sigma$ are elements of $\mathcal{V}_\sigma^0 \cup \mathcal{V}_\sigma$. We denote by

$$\mathcal{V} = \bigcup_{K\in\mathcal{M}}\bigcup_{\sigma\in\mathcal{E}_K}\mathcal{V}_\sigma.$$

For any $K \in \mathcal{M}$, $\sigma \in \mathcal{E}_K$, $\tau \in \mathcal{S}_\sigma$, we denote by $S_{K,\tau}$ the d-simplex (triangle if $d=2$, tetrahedron if $d=3$) with vertex $\boldsymbol{x}_K$ and basis τ.

- We then define $X_{\mathcal{D}}$ as the set of all families $u = ((u_K)_{K\in\mathcal{M}}, (u_{\boldsymbol{v}})_{\boldsymbol{v}\in\mathcal{V}})$ and $X_{\mathcal{D},0}$ the set of all families $u \in X_{\mathcal{D}}$ such that $u_{\boldsymbol{v}} = 0$ for all $\boldsymbol{v} \in \mathcal{V} \cap \partial\Omega$.
- The mapping $\Pi_{\mathcal{D}}$ is defined, for any $u \in X_{\mathcal{D}}$, by $\Pi_{\mathcal{D}} u(\boldsymbol{x}) = u_K$, for a.e. $\boldsymbol{x} \in K$.
- The mapping $\nabla_{\mathcal{D}}$ is defined, for any $u \in X_{\mathcal{D}}$, by $\nabla_{\mathcal{D}} u(\boldsymbol{x}) = \boldsymbol{G}_{K,\tau}$, for all $\sigma \in \mathcal{E}_K$ and $\tau \in \mathcal{S}_\sigma$, and for a.e. $\boldsymbol{x} \in S_{K,\tau}$, where $\boldsymbol{G}_{K,\tau} \in \mathbb{R}^d$ is the gradient of the affine function whose values are u_K at $\boldsymbol{x}_K$, $u_{\boldsymbol{v}}$ at any vertex $\boldsymbol{v}$ of τ which belongs to $\mathcal{V}_\sigma$, and $\sum_{\boldsymbol{x}\in\mathcal{V}_\sigma} \alpha_{\boldsymbol{v}}^{\boldsymbol{x}} u_{\boldsymbol{x}}$ at any vertex $\boldsymbol{v}$ of τ which belongs to $\mathcal{V}_\sigma^0$.

It is then proved in [16, 17] that this scheme allows to define a consistent sequence of space-time gradient discretisations in the sense of Definition 2.9, such that the associated sequence of approximate gradient approximations is coercive (Definition 2.3), limit–conforming (Definition 2.6) and compact (Definition 2.7), and such that, for all $m \in \mathbb{N}$, $\Pi_{\mathcal{D}_m}$ is a piecewise constant function reconstruction in the sense of Definition 2.10.
In the case of multiphase flows simulations, we define, between a cell and one of its vertices, a Darcy flux of a phase as described in details in [18]. The advantage of this scheme is that it allows to eliminate all values $(u_K)_{K\in\mathcal{M}}$ with respect to the values $(u_{\boldsymbol{v}})_{\boldsymbol{v}\in\mathcal{V}}$, leading to linear systems which are well suited to domain decomposition and parallel computing.

5.2 A one dimensional test

The objective of this first test case is to study numerically the theoretical models introduced in this paper, in a framework where the set J includes two elements. Such tests have been the object of theoretical and numerical works [5, 7, 15]. We consider an immiscible incompressible two phase flow in the domain $\Omega = (0, 100)$ (oriented upwards in the vertical direction), and we consider $J = \{\alpha, \beta\}$ with $\Omega_\alpha = (0, 50)$ and $\Omega_\beta = (50, 100)$. The porosity $\Phi(\boldsymbol{x}) = 0.1$, and the permeability $\Lambda(\boldsymbol{x}) = 10^{-12}\mathrm{Id}$ are homogeneous and the same for both subdomains. The mobility functions of the two phases, say respectively oil and water, are given by

$$k_1(\boldsymbol{x}, s) = \frac{s + kr_{\min}}{\mu_1} \qquad \text{and} \qquad k_2(\boldsymbol{x}, s) = \frac{1 - s + kr_{\min}}{\mu_2}$$

where $\mu_1 = 0.005$ and $\mu_2 = 0.001$ are the viscosities of the phases, and $kr_{\min}$ is a strictly positive real number; hence Hypothesis (4g) is fulfilled since we have

$$k_{\min} = \min\left(\frac{kr_{\min}}{\mu_1}, \frac{kr_{\min}}{\mu_2}\right) = \frac{kr_{\min}}{\mu_1};$$

the influence of its value is discussed below. Notice that we impose the non-degeneracy assumption on the relative permeabilities kr_i (and not the mobilities k_i) since it is the first ones which naturally vanish. Moreover these data are unit-less and take values between 0 and 1. The vectors $\boldsymbol{g}_i$ are given by $\boldsymbol{g}_i = \rho_i \boldsymbol{g}$ where $\boldsymbol{g}$ is the gravity vector (with $\|\boldsymbol{g}\| = 10$) and ρ_i is the phase density with $\rho_1 = 800$ and $\rho_2 = 1000$. The functions S_j, which are the reciprocal functions of the capillary pressure of each subdomain, are defined by

$$S_j(q) = \min(\max(\frac{q - b_j}{a_j}, 0), 1), \tag{29}$$

with $a_\alpha = a_\beta = 10^{+5}$, $b_\alpha = 0$ and $b_\beta = 0.5\ 10^{+5}$. The Dirichlet boundary conditions $v(0, t) = v_0$ and $u(0, t) = v_0 + 0.3a_\alpha + b_\alpha$ are imposed at $\boldsymbol{x} = 0$, and the Dirichlet boundary conditions $v(100, t) = v_0 - 100\boldsymbol{g}_2$ and $u(100, t) = v(100, t) + b_\beta$ are imposed at $\boldsymbol{x} = 100$, for a given value v_0 (the problem being independent of this value). The initial difference of the two pressures is defined by

$$p_{\mathrm{ini}}(x) = \begin{cases} 0.3a_\alpha + b_\alpha & \text{if } \boldsymbol{x} \in \Omega_\alpha, \\ b_\beta & \text{if } \boldsymbol{x} \in \Omega_\beta. \end{cases}$$

We also compute an approximate solution to Richards' equation (1b)-(6), which is expected to provide results comparable to the full two-phase flow problem, since the water phase is the most mobile. Indeed we see in the

numerical results below that in the full two-phase flow problem, the water saturation remains sufficiently high, which leads to nearly constant pressures with respect to the time variable.
Two grids are used for the computations, a coarse grid with 20 cells, and a finer grid with 80 cells and two different approximations of the mobility terms are considered, the centered scheme and the upwind one. Figures 1 and 2 compare at a given time the solutions obtained for the oil saturation $s_{\mathcal{D}}$ along the vertical axis.

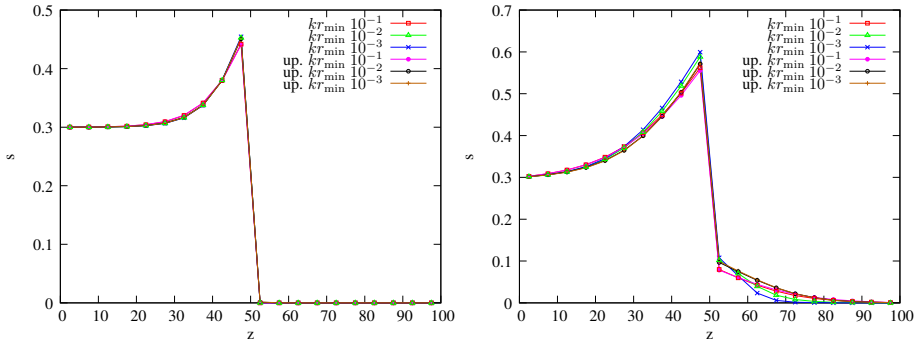

(a) 15 days - coarse grid

(b) 60 days - coarse grid

(c) 15 days - fine grid

(d) 60 days - fine grid

Figure 1: Oil saturation along the z axis after 15 and 60 days of simulation obtained for the **centered scheme** and the **upwind scheme** denoted by "up.".

Due to the imposed pressure at the boundaries, it is known that the oil should move to the top subdomain Ω_β provided that the capillary pressures can achieve continuity at the interface, meaning here that the jump of the oil saturation $s_{\mathcal{D}}$ at the interface must reach the value 0.5 before oil can move into the upper part. This is not achieved after 15 days of simulation, but is obtained at 60 days. We can observe that the results obtained with the upwind scheme and the centered scheme are very close, weakly dependent of the value of $k_{\min}$, and that they are already accurate on the coarse grid. As expected, the results obtained using the approximation of Richards' equation are also close to those obtained with the approximation of the full two-phase flow problem, as long as $k_{\min}$ remains sufficiently large.

5.3 Oil migration in a 2D basin with two barriers

We consider the simulation of the oil migration process, within a 2D cross section $\Omega = (0, L) \times (0, H)$, $H = L = 100\ m$ (see Figure 3). We denote by (x, y) the Cartesian coordinates of $\boldsymbol{x}$. We let again $J = \{\alpha, \beta\}$, with $\Lambda(\boldsymbol{x}) = 1.10^{-12}\mathrm{Id}$, $\Phi(\boldsymbol{x}) = 0.1$ and

$$k_1(\boldsymbol{x}, s) = \frac{s^2 + kr_{\min}}{\mu_1} \qquad \text{and} \qquad k_2(\boldsymbol{x}, s) = \frac{(1-s)^2 + kr_{\min}}{\mu_2}$$

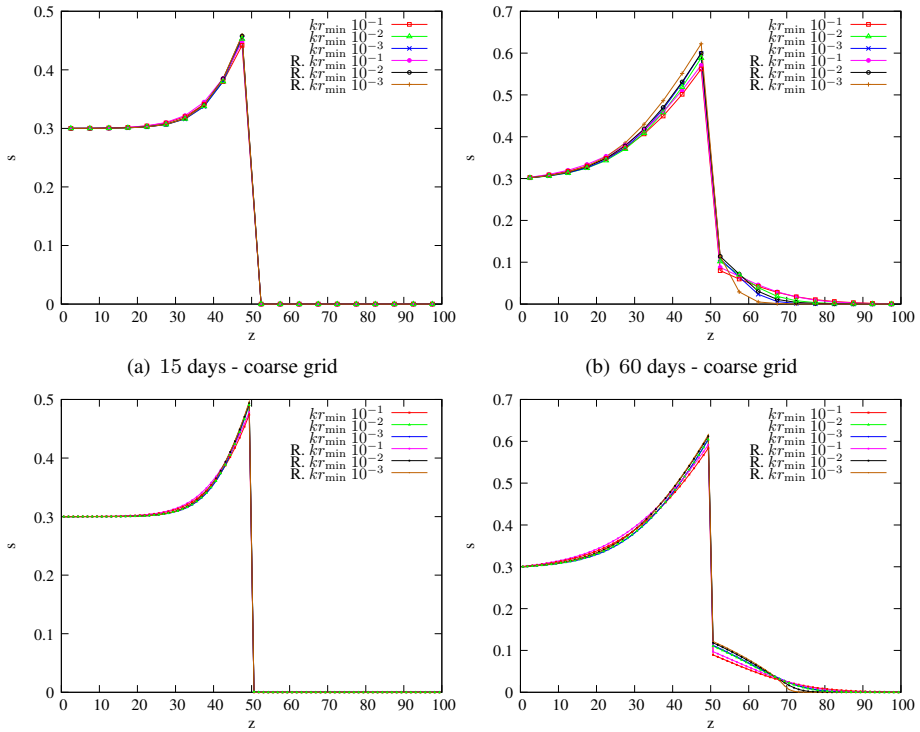

(a) 15 days - coarse grid

(b) 60 days - coarse grid

(c) 15 days - fine grid

(d) 60 days - fine grid

Figure 2: Oil saturation along the z axis after 15 and 60 days of simulation obtained for the **centered scheme** and Richards denoted by "R.".

where μ_i, $i = 1, 2$, is the viscosity of the phase i such that $\mu_1 = 0.005$ and $\mu_2 = 0.001$, and $kr_{\min}$ is a positive real value discussed below and again satisfies

$$k_{\min} = \frac{kr_{\min}}{\mu_1}.$$

The vectors $\boldsymbol{g}_i$ are given by $\boldsymbol{g}_i = \rho_i \boldsymbol{g}$ where $\boldsymbol{g}$ is the gravity vector (with $\|\boldsymbol{g}\| = 10$) and ρ_i is the phase density with $\rho_1 = 800$ and $\rho_2 = 1000$. and the functions $S_j(p)$ are given as in the 1D test case by (29) with $a_\alpha = a_\beta = 10^{+5}$, $b_\alpha = 0$ and $b_\beta = 0.5\ 10^{+5}$.
Neumann homogeneous boundary conditions are imposed at the right and left sides of Ω and Dirichlet boundary conditions are imposed on the top and bottom sides with $v(x, H, t) = 8.10^6\ Pa$, $u(x, H, t) - v(x, H, t) = b_\alpha\ Pa$, $v(x, 0, t) = v(x, H, t) + \rho_2 gH\ Pa$, $u(x, 0, t) - v(x, 0, t) = a_\alpha + b_\alpha\ Pa$ (input oil). The initial condition is defined by $p_{\text{ini}}(\boldsymbol{x}) = b_j, j \in \Omega_j, j \in J$.
The solution is first computed with the upwind scheme using $k_{\min} = 0$ on a uniform Cartesian coarse grid of size 16×16 exhibited in Figure 4. In that case the capillary pressure is not uniquely defined and can be viewed as a multivalued function (see [8], and [5]). In order to obtain a unique discrete solution and to solve the nonlinear system at each time step, the discrete capillary pressure at cell centers ($\boldsymbol{x} = \boldsymbol{x}_K, K \in \mathcal{M}$) and at the vertices ($\boldsymbol{x} \in \mathcal{V}$) will be projected on the interval $[\min_{\{j \in J \,|\, \boldsymbol{x} \in \bar{\Omega}_j\}} b_j, \max_{\{j \in J \,|\, \boldsymbol{x} \in \bar{\Omega}_j\}} b_j + a_j]$.
The oil saturation $s_{\mathcal{D}}$ is plotted at different times in Figure 4 on the submesh obtained by joining the midpoints of the successive edges of each cell. This submesh enables to plot all the values of $s_{\mathcal{D}}$ at a fixed time. Figure 4 clearly shows that the discrete oil saturation $s_{\mathcal{D}}$ satisfies the jump condition at the interface between the two rocktypes both at the entry and at the exit of the barriers. The comparison of $s_{\mathcal{D}}$ on the coarse grid at final time Figure 4 with the solutions $s_{\mathcal{D}}$ obtained on the refined meshes Figure 5 shows that the solution is already accurate on the coarse grid and that the results obtained on the Cartesian, quadrangular, and triangular fine meshes are very close.

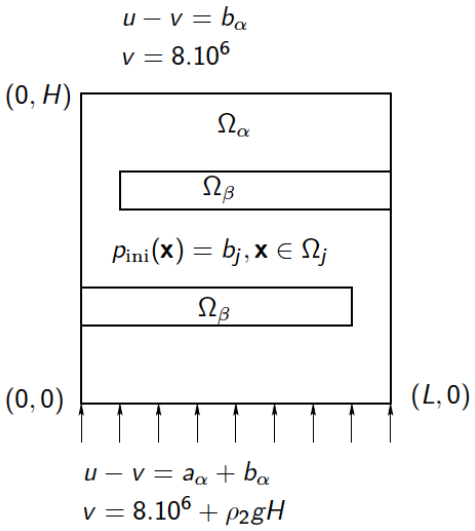

Figure 3: Test case with two barriers with rocktype β in the barrier and rocktype α outside.

Next, we compare Figure 6 the discrete oil saturation $s_{\mathcal{D}}$ obtained at final time on the 64×64 Cartesian grid for different values of $k_{\min}$. It shows that the the solution $s_{\mathcal{D}}$ obtained for $k_{\min} = 0.2$ (i.e. $kr_{\min} = 10^{-3}$) is already very closed to the one obtained for $k_{\min} = 0$.
To close the convergence study of this test case, we have plotted on the Figure 7 the discrete $L^2(\Omega)$ errors on each type of grids (these errors being computed at the final time). Since no analytical solution is available, we use as a reference solution the discrete solution obtained on a fine 512×512 Cartesian mesh. The error of each phase pressure is computed thanks to a bilinear interpolation and the saturation error is then deduced using its expression as a function of the capillary pressure. As expected, the order of convergence is at least one.

5.4 Oil migration in a 2D basin with random capillary pressure

The objective of this test case is to show the ability of the scheme to deal with many different rocktypes. The data for k_i, $\boldsymbol{g}_i$, Λ and Φ are the same as in the previous example. The capillary pressure curves are given by

$$S(\boldsymbol{x}, q) = \min(\max(\frac{q - \gamma(\boldsymbol{x})10^5}{10^5}, 0), 1),$$

where γ is a cellwise constant function with values chosen randomly in each cell in the interval $[-1, 1]$. Note that negative values of γ imply a change of wettability between the oil and water phases. As in the above case, we impose Neumann homogeneous boundary conditions on the right and left sides of Ω and Dirichlet boundary conditions on the top and bottom sides with $v(x, H, t) = 8.10^6\ Pa$, $u(x, H, t) - v(x, H, t) = \gamma(x, H)10^5\ Pa$, $v(x, 0, t) = v(x, H, t) + \rho_2 g H\ Pa$, $u(x, 0, t) - v(x, 0, t) = (1 + \gamma(x, 0))10^5\ Pa$ (input oil). The initial condition is defined by $p_{\text{ini}}(\boldsymbol{x}) = \gamma(\boldsymbol{x})10^5$. We can check in Figure 8 that the discrete oil saturation $s_{\mathcal{D}}$ follows mainly the paths of minimum $\gamma(\boldsymbol{x})$. We see on this test case the efficiency of the Vertex Approximate Gradient scheme and of the pressure formulation to handle the case of capillary-driven two-phase flow in random porous media, which represents for example the case where the values in each cell are generated by a homogenization process.

5.5 Oil migration in a 2D basin with barrier and fracture

We consider again the simulation of the oil migration process within the 2D cross section $\Omega = (0, L) \times (0, H)$, $H = L = 100\ m$. We denote by (x, y) the Cartesian coordinates of $\boldsymbol{x}$. We let again $J = \{\alpha, \beta\}$, with Ω_β the red

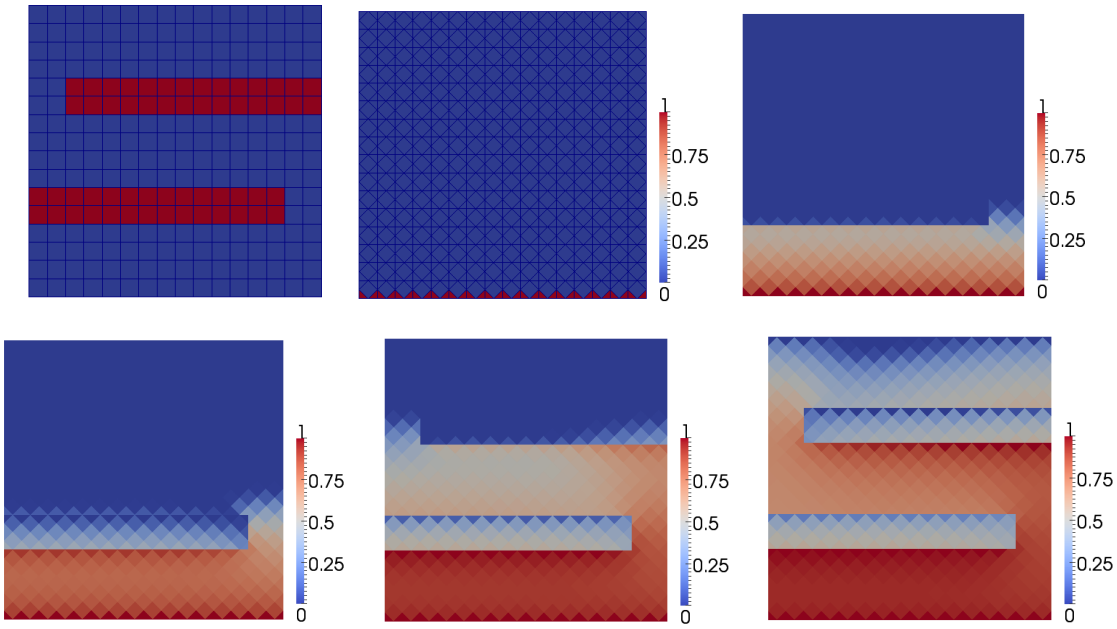

Figure 4: Cartesian mesh and discrete oil saturation $s_{\mathcal{D}}$ at successive times computed with the upwind scheme and $k_{\min} = 0$ on the 16×16 uniform Cartesian grid.

barrier exhibited in Figure 9 and $\Omega_\alpha = \Omega \setminus \overline{\Omega}_\beta$ the remaining subdomain in blue including the fracture Ω_f crossing the barrier. The porous media in $\Omega_\alpha \setminus \overline{\Omega}_f$ is assumed to be anisotropic, with a permeability tensor given by

$$\Lambda(\boldsymbol{x}) = \lambda_0 \begin{pmatrix} 0.82 & -0.36 \\ -0.36 & 0.28 \end{pmatrix}.$$

with $\lambda_0 = 10^{-12}$ m^2; the eigenvalues of Λ are $0.1\lambda_0$ and λ_0 and the corresponding eigenvectors are $(\frac{1}{\sqrt{5}}, \frac{2}{\sqrt{5}})$, $(\frac{2}{\sqrt{5}}, -\frac{1}{\sqrt{5}})$.
In the barrier subdomain Ω_β, the porous media is isotropic, with a permeability tensor $\Lambda(\boldsymbol{x}) = \frac{\lambda_0}{100} I$, and in the fracture subdomain Ω_f, the porous media is also assumed isotropic with a permeability tensor $\Lambda(\boldsymbol{x}) = 10\lambda_0 I$.
The vectors $\boldsymbol{g}_i$ are given by $\boldsymbol{g}_i = \rho_i \boldsymbol{g}$ where $\boldsymbol{g}$ is the gravity vector (with $\|\boldsymbol{g}\| = 10$) and ρ_i is the phase density with $\rho_1 = 850$ and $\rho_2 = 1000$.
The inverse of the capillary pressure monotone graph in each subdomain $\Omega_j, j \in J$ is defined by

$$S_j(q) = \begin{cases} 0 & \text{if } q < a_j, \\ (1 - s_{r2})(1 - e^{\frac{a_j - q}{b_j}}) & \text{if } q \geq a_j, \end{cases}$$

with the parameters $s_{r2} = 0.2$, $a_\beta = 2\ 10^5$ Pa, $a_\alpha = 10^5$ Pa, $b_\beta = 10^2$ Pa, and $b_\alpha = 10^4$ Pa.
The mobilities of the two phases are given by

$$k_1(s) = \begin{cases} 0 & \text{if } s < 0, \\ \frac{1}{\mu_1} & \text{if } s > 1 - s_{r2}, \\ \frac{s^2}{(1-s_{r2})^2 \mu_1} & \text{else}, \end{cases}$$

for phase 1 (oil), and

$$k_2(s) = \begin{cases} 0 & \text{if } s > 1 - s_{r2}, \\ \frac{1}{\mu_2} & \text{if } s < 0, \\ \frac{(1-s-s_{r2})^2}{(1-s_{r2})^2 \mu_2} & \text{else}, \end{cases}$$

for t phase 2 (water). Phase 1 is injected at the bottom boundary $(40, 60) \times \{0\}$ with imposed pressures $v = 8\ 10^6$ Pa, $u = v + S_\alpha^{-1}(0.2)$ corresponding to an input phase 1 saturation $s = 0.2$. All remaining boundaries are assumed to be impervious. At initial time the porous media is saturated with phase 2 with a hydrostatic pressure $v(\boldsymbol{x}) = 8\ 10^6 - \rho^w g y$, and a phase 1 pressure defined by $u(\boldsymbol{x}) = v(\boldsymbol{x}) + a_j$ for $\boldsymbol{x} \in \Omega_j$, $j \in J$.
The mesh is a 100×100 topologically Cartesian quadrangular grid , which is refined below the barrier. Figure 9 exhibits the oil (phase 1) saturation at a final simulation time of 4000 days. We clearly see that the oil phase rises by gravity along the direction of the highest permeability and accumulates below the barrier. Due to the saturation jump condition at the barrier drain interface given by the capillary pressures functions, oil can only cross the barrier through the fracture as can be checked in Figure 9.

5.6 Oil migration in a 3D basin with barriers

This case is a 3D extension of the 2D case with again two rocktypes $J = \{\alpha, \beta\}$. The mesh of the domain $\Omega \subset (0, 100\mathrm{m})^3$ exhibited Figure 10 is hexahedral with degeneracies of some hexahedra due to erosion leading to the collapse of up to three vertical edges of the cell. It includes three barriers of rocktype β exhibited in red in Figure 10. The remaining of the domain is of rocktype α. Note that the barrier located in the middle of the domain extends on the full domain horizontally while the two others extend only on the right horizontal side of the domain. The boundary conditions are the same as for test case 5.3 except on the bottom side for which oil is injected only on the right side below the first barrier.
The functions S_j, $j \in J$ are still defined by (29) with modified parameters $a_\alpha = a_\beta = 10^{+5}$, $b_\alpha = 0$ and $b_\beta = 1.5\ 10^{+5}$, and the densities are changed to $\rho_1 = 850$, $\rho_2 = 1000$. Other parameters are unchanged compared with test case 5.3. With this choice of the functions S_j, $j \in J$, the oil saturation can pass through the barrier only if it reaches 1 below the barrier and if the difference of pressure $u - v$ roughly given by $(\rho_2 - \rho_1)gh + a_\alpha + b_\alpha$ is larger than b_β where h is the vertical distance between the barrier and the bottom side. It results that oil will not go through the first barrier due to insufficient gravity load but can go through the second and the third ones.
This is what is observed in Figure 11 which exhibits the discrete oil saturation at final simulation time obtained for $k_{\min} = 0$ with the upwind scheme.
Figure 12 shows the diffusive effect of the parameter $k_{\min}$ which has a larger impact on the solution in that test case than in the previous ones due to the low saturation values at the exit of the barriers and to the large simulation time.

6 Conclusion

In this paper, we proved the convergence of a large class of numerical methods, namely the gradient schemes, for the two-phase flow problem. Our study includes an extended Richards model; this latter model is shown to give a precise approximation of the full two-phase flow problem for numerical examples taken from the oil engineering framework. Applications of the gradient schemes to other nonlinear problems, such as the Stefan problem, are the object of ongoing works. It is important to underline that the proof of convergence of general gradient schemes remains an open problem in the case where the estimates require the multiplication of the equations by nonlinear functions of the term involved in the discrete gradient: this is the case for instance when dealing with discontinuous capillary forces, or even for the standard two-phase flow problem but without assuming a lower bound on the relative permeabilities, or, equivalently, on the range of the saturation function. In these latter cases, the convergence proof [6, 7, 15, 19] is known for two point flux approximations, but it relies on the maximum principle which does not hold for gradient schemes.
Acknowledgement. The second and fourth authors acknowledge TOTAL's support for this work.

References

[1] O. Angelini, C. Chavant, E. Chénier, R. Eymard, and S. Granet. Finite volume approximation of a diffusion-dissolution model and application to nuclear waste storage. *Mathematics and Computers in Simulation*, 81(10):2001–2017, 2011.

[2] T. Arbogast. The existence of weak solutions to single porosity and simple dual-porosity models of two-phase incompressible flow. *Nonlinear Analysis: Theory, Methods & Applications*, 19(11):1009–1031, 1992.

[3] K. Aziz and A. Settari. *Petroleum Reservoir Simulation*. Applied Science Publishers, 1979.

[4] B. Belfort, F. Ramasomanana, A. Younes, and F. Lehmann. An efficient lumped mixed hybrid finite element formulation for variably saturated groundwater flow. *Vadose Zone Journal*, 8(2):352–362, 2009.

[5] K. Brenner, C. Cancès, and D. Hilhorst. A convergent finite volume scheme for two-phase flows in porous media with discontinuous capillary pressure field. In *Finite volumes for complex applications. VI. Problems & perspectives. Volume 1, 2*, volume 4 of *Springer Proc. Math.*, pages 185–193. Springer, Heidelberg, 2011.

[6] K. Brenner, C. Cancès, and D. Hilhorst. Finite volume approximation for an immiscible two-phase flow in porous media with discontinuous capillary pressure. 2012 (submitted).

[7] C. Cancès. Finite volume scheme for two-phase flows in heterogeneous porous media involving capillary pressure discontinuities. *M2AN Math. Model. Numer. Anal.*, 43(5):973–1001, 2009.

[8] C. Cancès and M. Pierre. An existence result for multidimensional immiscible two-phase flows with discontinuous capillary pressure field. *SIAM J. Math. Anal.*, 44(2):966–992, 2012.

[9] M. Celia, E. Bouloutas, and R. Zarba. A general mass-conservative numerical solution for the unsaturated flow equation. *Water Resources Research*, 26(7):1483–1496, 1990.

[10] G. Chavent. The global pressure, a new concept for the modelization of compressible two-phase flows in porous media. *In Flow and Transport in porous Media, A. Verruijt and F. Barends eds., Balkema,Proceedings of Euromech*, pages 191–198, 1981.

[11] C. Chen and V. Thomée. The lumped mass finite element method for a parabolic problem. *J. Austral. Math. Soc. Ser. B*, 26(3):329–354, 1985.

[12] Z. Chen. Degenerate two-phase incompressible flow: I. existence, uniqueness and regularity of a weak solution. *Journal of Differential Equations*, 171(2):203–232, 2001.

[13] J. Droniou, R. Eymard, T. Gallouët, and R. Herbin. A unified approach to mimetic finite difference, hybrid finite volume and mixed finite volume methods. *Math. Models Methods Appl. Sci.*, 20(2):265–295, 2010.

[14] J. Droniou, R. Eymard, T. Gallouët, and R. Herbin. Gradient schemes: a generic framework for the discretisation of linear, nonlinear and nonlocal elliptic and parabolic equations. *submitted*, 2012.

[15] G. Enchéry, R. Eymard, and A. Michel. Numerical approximation of a two-phase flow problem in a porous medium with discontinuous capillary forces. *SIAM J. Numer. Anal.*, 43(6):2402–2422 (electronic), 2006.

[16] R. Eymard, P. Féron, T. Gallouet, R. Herbin, and C. Guichard. Gradient schemes for the Stefan problem, `http://hal.archives-ouvertes.fr/hal-00751555` . *accepted for publication in Int. J. of Fin. Vol.*, 2013.

[17] R. Eymard, C. Guichard, and R. Herbin. Small-stencil 3d schemes for diffusive flows in porous media. *M2AN*, 46:265–290, 2012.

[18] R. Eymard, C. Guichard, R. Herbin, and R. Masson. Vertex-centred discretization of multiphase compositional darcy flows on general meshes. *Computational Geosciences*, pages 1–19, 2012.

[19] R. Eymard, R. Herbin, and A. Michel. Mathematical study of a petroleum-engineering scheme. *M2AN Math. Model. Numer. Anal.*, 37(6):937–972, 2003.

[20] G. Gagneux and M. Madaune-Tort. *Analyse mathématique de modèles non linéaires de l'ingénierie pétrolière*, volume 22 of *Mathématiques & Applications (Berlin) [Mathematics & Applications]*. Springer-Verlag, Berlin, 1996. With a preface by Charles-Michel Marle.

[21] A. Michel. A finite volume scheme for two-phase immiscible flow in porous media. *SIAM J. Numer. Anal.*, 41(4):1301–1317 (electronic), 2003.

[22] D. Peaceman. *Fundamentals of numerical reservoir simulation*, volume 6. Elsevier, 1977.

[23] D. Shi, H. Wang, and Z. Li. A lumped mass nonconforming finite element method for nonlinear parabolic integro-differential equations on anisotropic meshes. *Applied Mathematics-A Journal of Chinese Universities*, 24(1):97–104, 2009.

[24] F. Tracy. An accuracy analysis of mass matrix lumping for three-dimensional, unsaturated flow, finite element, porous media computations using analytical solutions. *PAMM*, 7(1):2020025–2020026, 2007.

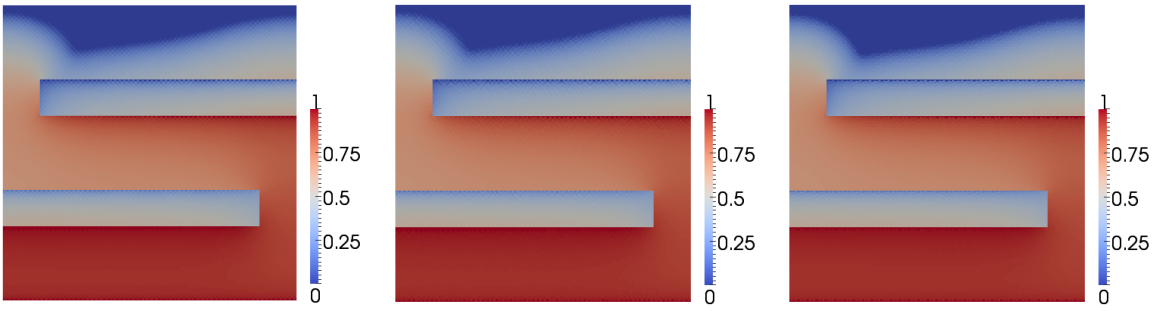

Figure 5: Comparison of the discrete oil saturation $s_{\mathcal{D}}$ at final time computed with the upwind scheme and $k_{\min} = 0$ on the uniform Cartesian 64×64, grid, a random quadrangular 64×64 mesh, and a triangular mesh with 7297 nodes.

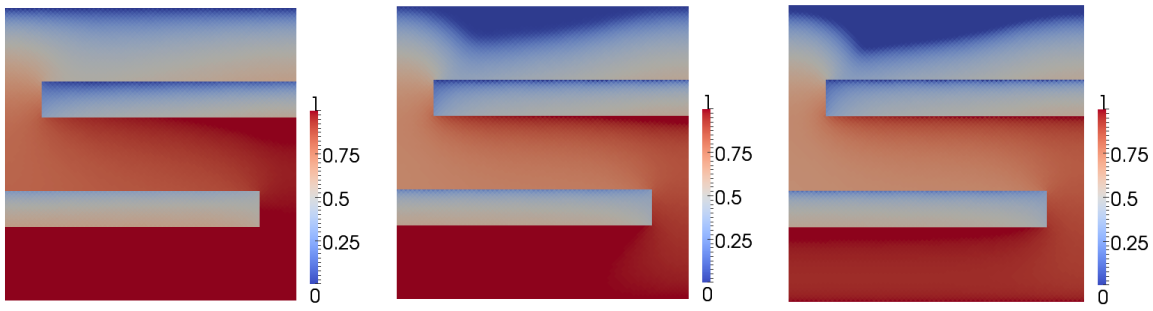

Figure 6: Comparison of the discrete oil saturation $s_{\mathcal{D}}$ at final time on the uniform Cartesian 64×64, mesh computed with the upwind scheme and different values of $kr_{\min} = 10^{-1}, 10^{-2}, 10^{-3}$ (which implies here $k_{\min} = 20,\ 2,\ 0.2$) from left to right.

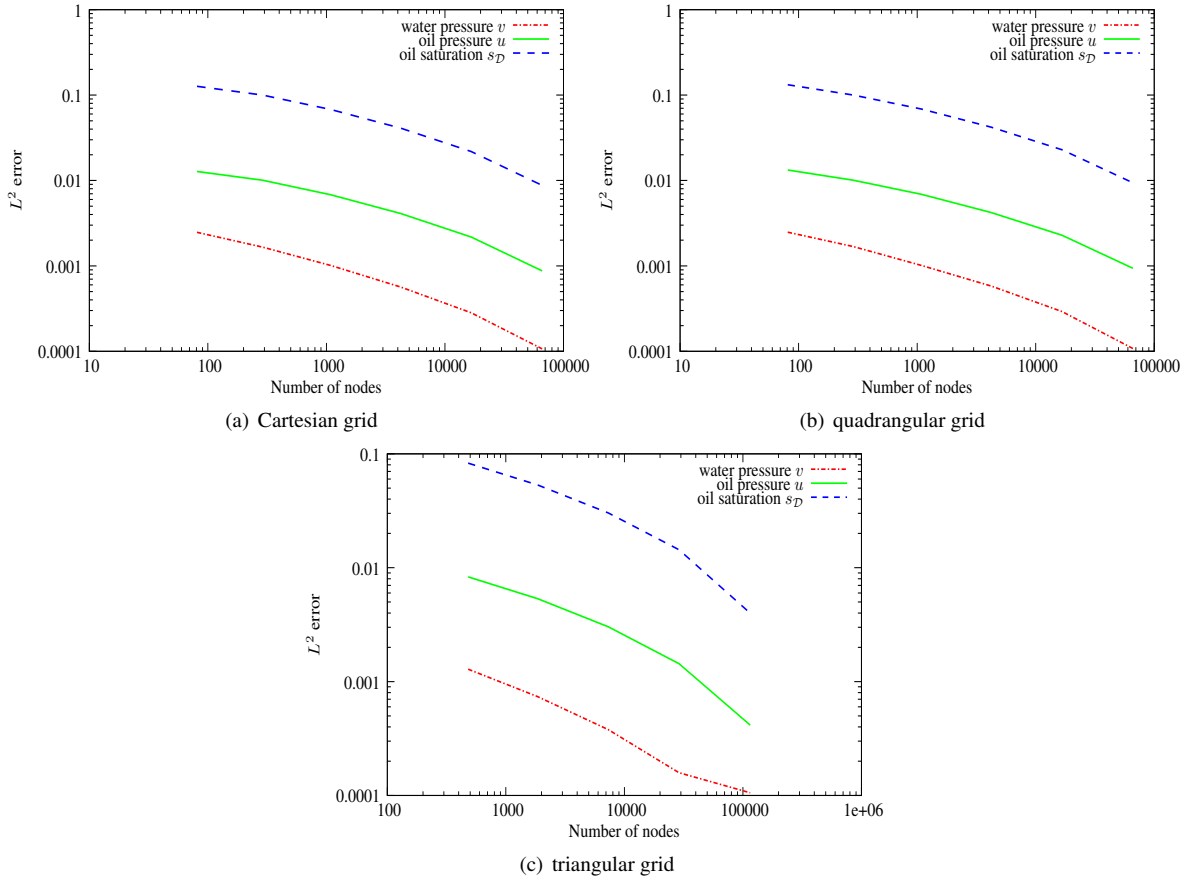

(a) Cartesian grid

(b) quadrangular grid

(c) triangular grid

Figure 7: convergence of discrete $L^2(\Omega)$ errors at the final time on different grids using as reference the discrete solution of the Cartesian mesh with 512×512 cells.

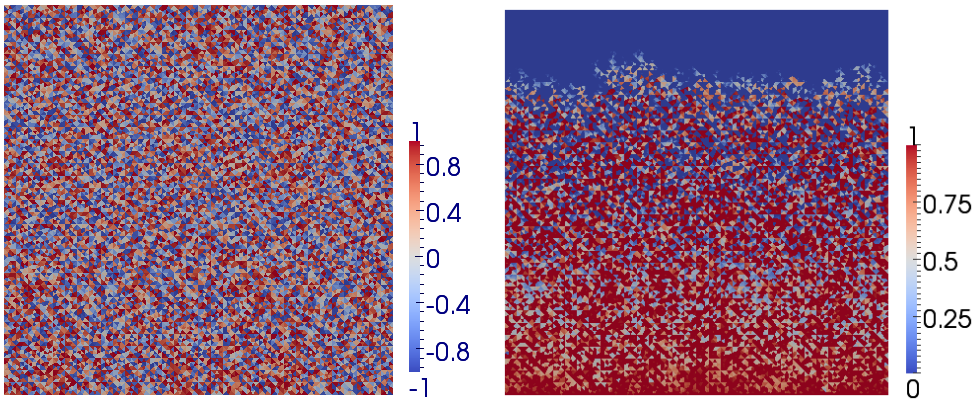

Figure 8: Cellwise constant parameter γ for the rocktype on the triangular mesh with 7297 nodes (left) and discrete oil saturation $s_{\mathcal{D}}$ computed with the upwind scheme for $k_{\min} = 0$ with this random capillary pressure.

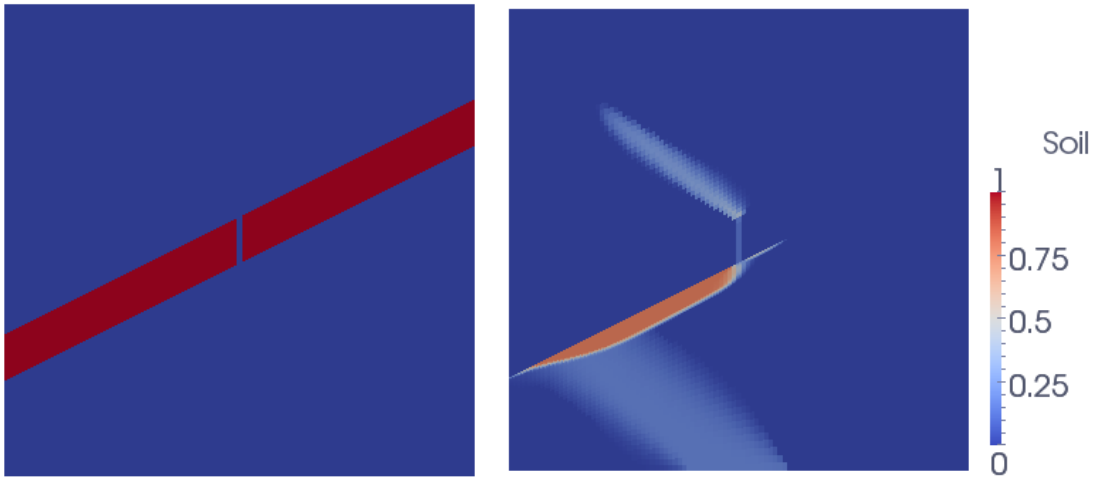

Figure 9: 2D basin with one barrier in red and a fracture crossing the barrier. Oil saturation (phase 1) after 4000 days of simulation on a 100×100 quadrangular mesh obtained with the upwind scheme.

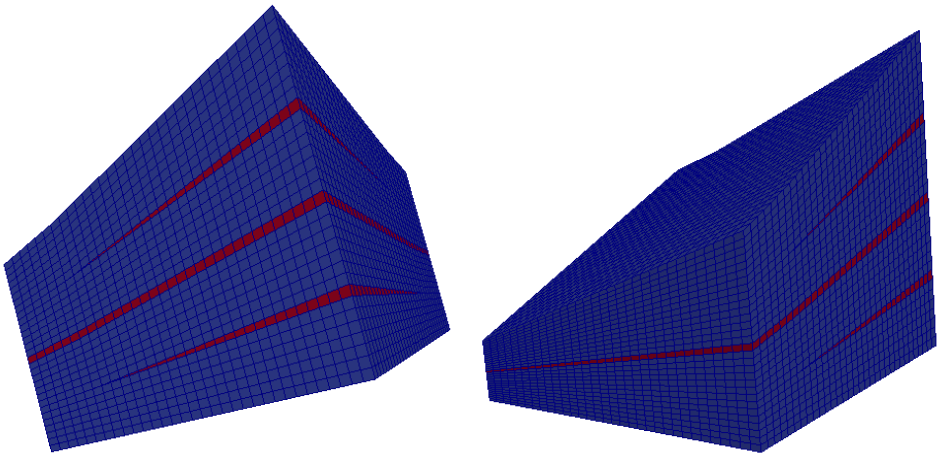

Figure 10: Hexahedral mesh (with degeneracies of some hexahedra due to erosion) of the domain with the three barriers in red (rocktype β in the red barriers and α outside the barriers).

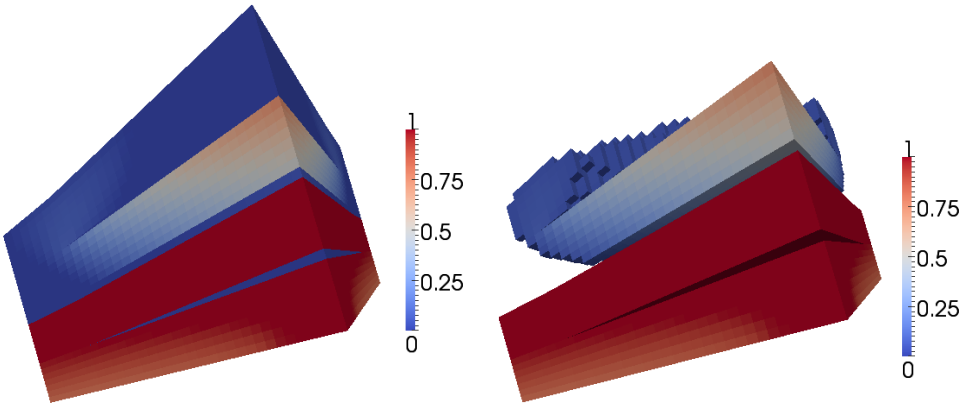

Figure 11: Discrete oil saturation $s_{\mathcal{D}}$ at final time computed with the upwind scheme and $k_{\min} = 0$. On the right side plot of the oil saturation at final time for $s_{\mathcal{D}} > 0.05$

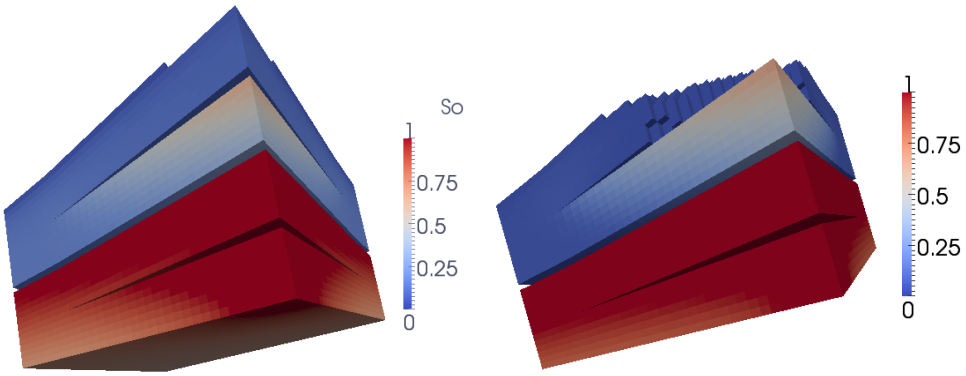

Figure 12: Plot of the oil saturation at final time for $s_{\mathcal{D}} > 0.05$ computed with the upwind scheme and $kr_{\min} = 10^{-3} \Rightarrow k_{\min} = 0.2$ (left) and $kr_{\min} = 10^{-4} \Rightarrow k_{\min} = 0.02$ (right).